Ttrap is an essential modulator of Smad3-dependent Nodal signaling during zebrafish gastrulation and left-right axis determination

Camila V. Esguerra[1,2,*,†], Luc Nelles[3,4,‡], Liesbeth Vermeire[3,4], Abdelilah Ibrahimi[3,4,§], Alexander D. Crawford[1,2,¶], Rita Derua[5], Els Janssens[1,2], Etienne Waelkens[5], Peter Carmeliet[1,2], Desiré Collen[1,2] and Danny Huylebroeck[3,4,*]

During vertebrate development, signaling by the TGFβ ligand Nodal is critical for mesoderm formation, correct positioning of the anterior-posterior axis, normal anterior and midline patterning, and left-right asymmetric development of the heart and viscera. Stimulation of Alk4/EGF-CFC receptor complexes by Nodal activates Smad2/3, leading to left-sided expression of target genes that promote asymmetric placement of certain internal organs. We identified Ttrap as a novel Alk4- and Smad3-interacting protein that controls gastrulation movements and left-right axis determination in zebrafish. Morpholino-mediated Ttrap knockdown increases Smad3 activity, leading to ectopic expression of *snail1a* and apparent repression of *e-cadherin*, thereby perturbing cell movements during convergent extension, epiboly and node formation. Thus, although the role of Smad proteins in mediating Nodal signaling is well-documented, the functional characterization of Ttrap provides insight into a novel Smad partner that plays an essential role in the fine-tuning of this signal transduction cascade.

KEY WORDS: Alk4, E-cadherin, Gastrulation, Left-right asymmetry, Node, Smad

INTRODUCTION

Nodal is the major signal in the establishment of left-right (LR) asymmetry during vertebrate development (Reissmann et al., 2001; Schier, 2003; Yost, 2003; Raya and Belmonte, 2004). The binding of Nodal to its receptor complex (Alk4/ActRIIB/co-receptor EGF-CFC) activates Smad2/3, and phosphorylation of these Smads by Alk4 increases their affinity for Smad4. The resulting Smad complexes accumulate in the nucleus and participate in transcription of target genes by cooperating with various activators, repressors and chromatin modulators (Massagué, 2000; van Grunsven et al., 2005).

The best characterized Smad2/3 partners in Nodal-Activin signaling (Stemple, 2000) are FoxHI (Fast1) and Mixer (Hill, 2001; Whitman, 2001; Attisano, 2001). Analysis of zebrafish mutants for FoxHI (*schmalspur*, *sur*) (Pogoda et al., 2000) and Mixer-like (*bonnie and clyde*, *bon*) (Kikuchi et al., 2000) revealed that the individual and combinatorial mutant phenotypes do not represent all aspects of Nodal signaling (Kunwar et al., 2003). This could be due

to several reasons, including the possibility that additional players in Smad signaling remain to be identified. Nodal signaling studies in fish have focused on the role of Smad2/FoxHI and identification of its targets, whereas the situation is less clear with regard to Smad3 (complexes).

Within the context of an antisense screen in zebrafish using morpholino oligomers (morpholinos, Mos) (Summerton and Weller, 1997; Nasevicius and Ekker, 2000), we identified Ttrap (TRAF and TNF receptor-associated protein) (Pype et al., 2000) as a regulator of embryogenesis. Human TTRAP interacts with TNF receptor (TNFR) family members and TNFR-associated factors (TRAFs) and inhibits NF-κB activation in TTRAP-overproducing cells (Pype et al., 2000). TTRAP has also been termed EAPII – ETS-associated protein II – revealing a possible dual role of this protein within the cytoplasm and nucleus (Pei et al., 2003). TTRAP belongs to the family of divalent cation-dependent phosphodiesterases, with highest homology to APE1, an endonuclease involved in DNA repair and transcription factor activation (Rodrigues-Lima et al., 2001).

The in vivo role of Ttrap has not yet been described. We show that Ttrap controls gastrulation movements and LR axis determination in zebrafish via Smad3-mediated regulation of *e-cadherin*, which is known to be regulated by the repressor snail and modulate cell movements (epiboly and convergent extension) in fish embryos (Babb and Marrs, 2004; Kane et al., 2005; Shimizu et al., 2005). We also uncovered a possible role for *e-cadherin* in the organization of dorsal forerunner cells (DFCs) during formation of Kupffer's vesicle (KV), a signaling center essential for establishing LR asymmetry.

MATERIALS AND METHODS

Zebrafish husbandry
Danio rerio stocks were maintained at 28.5°C under standard aquaculture conditions. Embryos were staged by hours post fertilization (hpf) using staging criteria as described (Westerfield, 1995).

[1]Center for Transgene Technology and Gene Therapy, VIB, [2]Department of Molecular and Cellular Medicine, KULeuven, [3]Laboratory of Molecular Biology, Department of Molecular and Developmental Genetics, VIB, [4]Department of Human Genetics, KULeuven, [5]Division of Biochemistry, Department of Molecular Cell Biology, KULeuven, Herestraat 49, B-3000 Leuven, Belgium.

*Authors for correspondence (e-mails: camila.esguerra@med.kuleuven.be; danny.huylebroeck@med.kuleuven.be)
†Present address: Stem Cell Institute Leuven (SCIL), KULeuven, Herestraat 49, B-3000 Leuven, Belgium
‡Present address: Galapagos, Generaal De Wittelaan L11A3, B-2800 Mechelen, Belgium
§Present address: Laboratory for Molecular Virology and Gene Therapy, Department of Molecular and Cellular Medicine, KULeuven, Kapucijnenvoer 33, B-3000 Leuven, Belgium
¶Present address: Department of Pharmaceutical Sciences, KULeuven, Herestraat 49, B-3000 Leuven, Belgium

Cloning of zebrafish *ttrap*, morpholinos and mRNA overexpression

A cDNA encoding full-length Ttrap (DQ524846) was isolated from a 5′cap-selected, normalized zebrafish embryo cDNA library by EST screening. It is 24 bp longer at the 5′ end than two other *ttrap* cDNAs (BC083404, BC097117, GenBank). MOs and mRNAs were injected into 1- to 2-cell-stage embryos. Plasmids containing cDNAs were linearized, column purified and subjected to in vitro transcription (Ambion mMessage mMachine High Yield Capped RNA kit), followed by poly(A)-tailing. For DFC-specific knockdowns, embryos were injected into the yolk between 2 and 4 hpf with fluorescence-tagged MOs. The degree of fluorescence in DFCs and forming KV were visually controlled using microscopy. For MOs used in this study, see Table S1 in the supplementary material.

Antisense morpholino oligomer screen

Around 3000 antisense morpholino oligomers (MOs) targeting the putative start codons and/or 5′ untranslated regions (UTRs) of zebrafish mRNAs were designed using GenBank cDNA sequences and 5′ expressed sequence tags (ESTs) generated from normalized, full-length (5′ cap-selected) cDNA libraries encompassing various developmental stages and adult tissues. Targeted sequences were selected randomly. For all MOs that induced a phenotype at one concentration, additional concentrations were tested in a second round of screening (concentration range: 1-8 ng). A second MO (non-overlapping with the first MO sequence) was designed for each gene that was deemed 'interesting' based on knockdown phenotype, protein structure, and functional data, and tested again for phenotypic specificity. For the screen in which TTRAP was initially identified as affecting vascular development, MO-injected embryos were subjected to in situ hybridization analysis at 28 hpf using a *flk1* probe and subsequently in separate knockdown experiments analyzed by live imaging to observe blood flow and outgrowth of vessels.

Whole-mount in situ hybridization analysis

In vitro transcription of digoxigenin-RNA probes and whole-mount in situ hybridization were performed according to Hauptmann and Gerster (Hauptmann and Gerster, 1994).

Microscopy and photodocumentation

Embryos were scored manually using light and fluorescence stereomicroscopy [Stemi-2000C and Lumar V12 (Zeiss), and MZ100FLIII (Leica)]. Digital images were captured using an AxioCam MRc5 and processed with Axiovision 4.5 Software (Zeiss).

Whole-embryo qRT-PCR

For qRT-PCR, 15-20 embryos were pooled and RNA extracted (Tri-pure, Roche) and purified (RNeasy RNA purification columns, Qiagen). RNA extraction on single embryos was performed in a similar fashion. RT was performed using MuMLV reverse transcriptase (Revert-aid, Fermentas), oligo-dT and random primers. Real-time qPCR on single embryos was performed on ABI7000 using the SYBRgreen amplification reagent (Eurogentec). For *cdh1*, we used PCR primers: F, 5′-ATGATGTGGC-GCCCACTTT-3′ and R, 5′-CCGGTCGAGGTCTGTACTGAG-3′. PCR on whole-embryo cDNA was performed with primers: F, 5′-TGCTCATT-GCTCAGGTGACTTT-3′ and R, 5′-TTCTTGTTTGCCCAGCTGTTC-3′ to amplify a 251-bp region of *ttrap* cDNA, and primers: F, 5′-GCCTTC-CTTCCTGGGCATGG-3′ and R, 5′-CCAAGATGGAGCCACCGAT-3′ for a 251-bp region of β-actin cDNA.

Protein studies

To check wild-type and mutant TTRAP synthesis, 250 pg of mRNA made from pCS2-huTTRAP or pCS2-huTTRAP^{T88A,T92A} were injected into one-cell embryos. To test the efficacy of knockdown in vivo, 80 pg mRNA from pCDNA3-HA-zfttrap were injected either alone or together with 16 ng Ttrap^{SCMO} or Ttrap^{MO}. Western blot analysis was carried out on sonicated extracts from 20-30 pooled embryos; extracts were immunoblotted and proteins detected using anti-TTRAP, anti-HA or anti-tubulin antibodies.

Co-immunoprecipitation assays

2 μg MycAlk4-pCDNA3 or HA-Smad2/3/4-pCDNA3 were transfected into HEK293T cells, together with 2 μg FlagTTRAP-pCS2 or FlagTTRAP-frame-shift-pCS2 (control). Co-immunoprecipitation studies of FlagTTRAP with Alk4 and Smads were performed as described (Pype et al., 2000). To test the interaction between TTRAP and Smad3, HEK293T cells were transfected with 2 μg TTRAP-pCS3 or TTRAP^{T88A,T92A}-pCS3 together with either HA-Smad3-pCDNA3 or FlagTTRAP-frame-shift-pCS2 (control).

Luciferase reporter assays

Reporter constructs were injected into the cytoplasm of one-cell embryos. From a large collection of injected embryos, 15-20 (one set) were randomly selected and re-injected with 16 ng Ttrap^{MO} and control^{MO}. Embryos were allowed to develop to shield stage, lysed (100 μl passive lysis buffer, Promega) and 10 μl lysate was aliquoted in triplicate into 96-well plates. Lysates were incubated with two volumes luciferin (Promega) and measured for luciferase activity. The readouts from one triplicate set were averaged and treated as one data point. Fold induction was calculated by dividing the mean value for Ttrap^{MO} by the mean value for control^{MO} embryos. The pGL3 control assay was performed three times and the ARE-luciferase assay eight times. Statistical analysis was with the Student's unpaired *t*-test. The same conditions for experiments +/– *sqt* or *cyc* RNA were used (see above), and measurements performed in triplicate. Statistical analysis was carried out using ANOVA (One-way analysis of variance).

Alk4 kinase assay

Strep-TTRAP-Myc-His was purified from HEK293T cells (Streptactin beads, IBA, Göttingen) and incubated with 250 ng Alk4 (Upstate, Lake Placid) and [γ-^{32}P]ATP for 10 minutes at 30°C. The reaction product was separated by PAGE, blotted and exposed to film. For in vivo phosphorylation, pStrepTTRAPMycHis was transfected into HEK293T cells with or without an expression vector encoding constitutively active Alk4. TTRAP was isolated using Ni-affinity purification under denaturing conditions.

Liquid chromatography mass spectrometry analysis

PhosphoTTRAP was reduced (10 mM DTT, 45 minutes, 60°C), alkylated (35 mM iodoacetamide, 30 minutes, 24°C; 15 mM DTT, 30 minutes, 24°C) and separated from contaminating proteins by 10% tricine SDS-PAGE. The band of interest was excised and the protein digested (trypsin, overnight, 37°C). The resulting peptide mix was analysed by nanoLC-MS/MS, consisting of a precursor 79(–) ion scan to signal the presence of putative phosphopeptides and a product(+) ion scan to determine the phosphorylated residue. Nano LC-MS/MS was performed on a Dionex Ultimate capillary liquid chromatography system coupled to an Applied Biosystems 4000 QTRAP mass spectrometer. Peptides were separated on a PepMap C18 column developed with a 30 minute linear gradient (0.1% formic acid, 6% acetonitrile/water-0.1% formic acid, 40% acetonitrile/water).

RESULTS

Ttrap was initially identified in a screen on the basis of defects in cardiovascular development, as visualized by in situ hybridization for *flk1* (Liao et al., 1997) and live analysis in the endothelium-specific transgenic eGFP line *Tg(fli1:egfp)y1* (Lawson and Weinstein, 2002). In addition to vascular outgrowth defects, zebrafish embryos with a MO-mediated knockdown of Ttrap (Ttrap^{MO}) displayed pericardial edemas and abnormal blood circulation in trunk and tail (not shown). These abnormalities were consistently associated with other gross morphological defects, prompting us to titer MO doses in an attempt to uncouple dysmorphology from vasculature defects. Closer inspection of Ttrap morphants uncovered heart-looping defects, suggesting its involvement in LR patterning.

Ttrap is essential for LR-axis determination and gastrulation

Ttrap^{MO} embryos (4 ng) displayed hallmarks of perturbed LR patterning. Observation of live embryos and whole-mount in situ hybridization (WISH) using *cardiac myosin light chain 2* (*cmlc2*) (Yelon et al., 1999) revealed that 64% of Ttrap^{MO} embryos exhibited
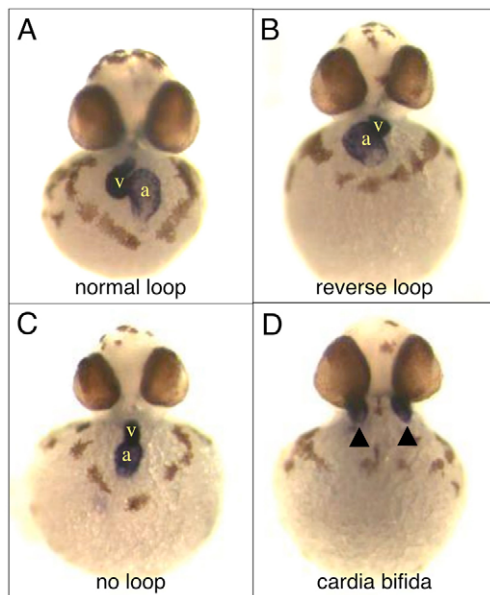
Fig. 1. Ttrap knockdown affects heart looping. Hearts were visualized via WISH for *cmlc2* at 48 hpf. (**A**) Control embryo, normal heart looping. (**B-D**) Ttrap[MO] embryos with reversed heart looping, no looping or cardia bifida. Arrowheads depict bilateral hearts in D. Frontal views; a, atrium; v, ventricle.

either reversed or no heart looping and occasionally cardia bifida by 48 hpf (Fig. 1; Table 1). We also scored Ttrap[MO] embryos at 28 hpf, before morphological chamber specification. In these embryos, the direction of heart jogging was also randomized (Table 2). This indicates that the heart looping defects were not simply due to improper cardiac differentiation but rather to either a general defect in LR-axis determination or failure of cardiac primordial cells to read LR positional cues.

All three MOs, which target different regions of the Ttrap transcript (see Table S1 in the supplementary material), induced heart looping defects (see Table S2 in the supplementary material). A subset of embryos also displayed gastrulation defects (thickened germ ring) for all MOs tested singly (see Table S3 in the supplementary material). A higher penetrance of gastrulation defects was obtained with a 1:1 mix of MO1 (8 ng) and MO2 (8 ng). This mix induced thickening of the germ ring in 40-72% (separate experiments) of shield-stage embryos (Fig. 2A,B). Up to half of

such embryos possessed a less distinct or absent shield. This combinatorial MO dose reduced Ttrap levels significantly (see Fig. S1 in the supplementary material). The phenotype could be partially rescued by injection of human (hu) *TTRAP* mRNA (see Table S4 in the supplementary material). The gastrulation defect is reminiscent of that observed in embryos where Nodal signaling is perturbed, particularly those with a knockdown of *lefty1* and *lefty2*, which results in unrestricted Nodal signaling in the organizer (Feldman et al., 2002). The lack of a shield has also been reported for the homozygous Nodal mutant *squint* (*sqt*) (Dougan et al., 2003).

The germ ring defect was followed by incomplete convergent extension (CE) movements as determined by analysis of *paraxial protocadherin* (*papc*) (Yamamoto et al., 1998) and *myogenic differentiation* (*myod*) (Weinberg et al., 1996), marking paraxial and adaxial mesoderm, respectively (Fig. 2C-F). Epiboly was also hampered in Ttrap[MO] embryos, with some undergoing yolk cell lysis between late gastrula stage (90% epiboly) and early somitogenesis (not shown). This lysis was probably caused by constriction of marginal cells in their attempt to achieve blastopore closure, despite their 'regressed' position relative to the vegetal pole (Fig. 2I). Of the embryos that did not undergo yolk cell lysis, some managed to achieve full or partial (Fig. 2H) blastopore closure. Ttrap[MO] embryos (Fig. 2K) displayed a shortened anterior-posterior axis, microcephaly, micropthalmia, and high incidence of pericardial edemas at 24 hpf, and cardia bifida (not shown) by 48 hpf. Together, these later phenotypes are similar to those resulting from CE movement defects (Matsui et al., 2005). The cardiac looping phenotype is unlikely to result from a general perturbation of gastrulation movements because at a lower MO dose (4 ng), the looping defects and cardia bifida were still observed in normally gastrulating embryos.

As depletion of Ttrap might also have randomized organ situs, we tested markers normally expressed left of the midline and markers of visceral organs (Fig. 3; Table 3): *bone morphogenetic protein-4* (*bmp4*) for cardiac primordium (Chen et al., 1997; Schilling et al., 1999), *paired-like homeodomain transcription factor-2* (*pitx2*) (Bisgrove et al., 1999; Campione et al., 1999) and *southpaw* (*spaw*) for left lateral plate mesoderm (LPM) (Long et al., 2003), *forkhead box-A3* (*foxA3*) for liver, pancreas, gut (Odenthal and Nusslein-Volhard, 1998; Alexander et al., 1999), and *lefty1* (*lft1*) for the left dorsal diencephalon (Liang et al., 2000) (Fig. 3). These markers were either absent or visibly reduced in level of expression, expressed bilaterally or on the right side in Ttrap[MO] embryos (Fig. 3A-E,F). LR-asymmetry defects were therefore not restricted to the heart, but observed along the entire rostral-caudal axis.

Table 1. Ttrap knockdown randomizes direction of heart looping

ISH marker	Stage	Morpholino	Dose	Total *n*	Normal	Reverse	No looping	Cardia bifida	Rudiments*	χ^2	$P \geqslant$
cmlc2	48 hpf	control MO	4 ng	54	94%	2%	4%	0%	0%	37.8	0.001
		ttrap MO	4 ng	44	36%	9%	45%	2%	7%		

*The term 'rudiments' is used for hearts that were strongly reduced in size, had no clearly discernable chambers, had not descended down onto the yolk sac, and were often only recognizable as 'hearts' because of their contractile behavior. These defects as well as the cardia bifida phenotype precluded the ability to score for direction of heart looping or jogging. Data presented is combined from two separate experiments. Chi-square analysis: Ttrap[MO] vs control[MO]; total no. of normal embryos vs total no. of embryos with looping defects.

Table 2. Ttrap knockdown randomizes direction of heart jogging

ISH marker	Stage	Morpholino	Dose	Total *n*	Normal	Reverse	No jogging	Cardia bifida	Rudiments*	χ^2	$P \leqslant$
cmlc2	28 hpf	control MO	4 ng	44	94%	2%	4%	0%	0%	39.5	0.001
		Ttrap MO	4 ng	38	29%	26%	24%	18%	3%		

*These defects (see Table 1) precluded ability to score for direction of heart looping. Data presented are combined from two separate experiments. Chi-square analysis: Ttrap[MO] vs control[MO]; total no. of normal embryos vs total no. of embryos with jogging defects.
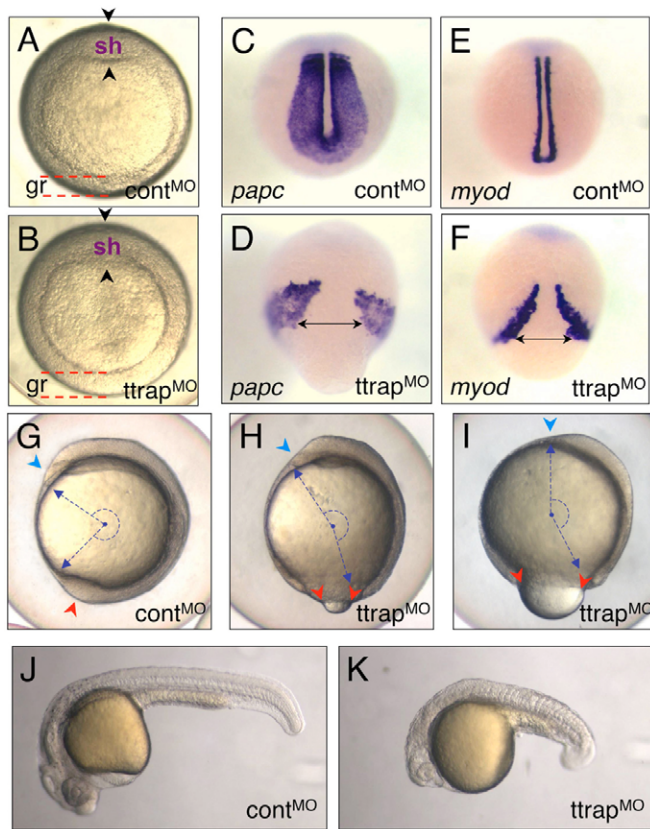
Fig. 2. Ttrap knockdown with higher MO dose induces gastrulation defects. (**A**,**B**) Ttrap[MO] embryos (B) with thickened germ ring at shield stage and a less distinct shield (arrowheads) than control (A). Animal views, dorsal on top (gr, germ ring; sh, shield). (**C-F**) *ttrap* is essential for CE movements. *papc/myod*-marked paraxial mesoderm cells fail to converge close to the midline in Ttrap[MO] embryos (D,F). Dorsal-posterior views, tailbud stage. Double-headed arrows depict width between cells spanning the midline. (**G-I**) *ttrap* is required during epiboly. (G) Control embryo (3 ss) showing blastopore closure (red arrowhead) and normal head with polster (blue). (H,I) Ttrap[MO] embryos (3 ss) showing varying degrees of severity with respect to epibolic movements. (H) Ttrap[MO] embryo displaying mild epiboly defect (red arrowheads), which shows only slightly open blastopore and relatively normal head morphology with polster (blue). (I) Ttrap[MO] embryo with more severe epiboly defect and larger open blastopore (red arrowheads). Downward spread of blastoderm cells only covers 80% of yolk cell; many of these embryos lyse shortly after; head region severely reduced in size with polster missing (blue arrowhead). The combination of CE and epiboly defects leads to severely truncated embryos. Blue dashed arrows and semi-circle depict embryo length and angle between anterior-posterior (AP) ends. Lateral views, dorsal to the right. (**J**,**K**) Live control[MO] versus Ttrap[MO] embryo, 24 hpf. The morphant embryo displays AP-axis truncation, microcephaly and micropthalmia.

The observed phenotypes suggest a role for Ttrap in signaling of Nodal or perhaps Bmp (Whitman and Mercola, 2001; Branford and Yost, 2004; Kishigami and Mishina, 2005). However, a direct involvement of Ttrap, at least in early Bmp signaling, is less likely because dorsal-ventral patterning did not appear to be affected in Ttrap[MO] embryos, as evidenced by morphological assessment and normal expression of *chordin* and *bmp2b* (not shown).

ttrap mRNA is expressed in Kupffer's vesicle and is required for node formation

We analyzed *ttrap* expression via RT-PCR (Fig. 4A) and WISH (Fig. 4B-E). Transcripts were detected in all blastomeres during cleavage stages, indicating that *ttrap* mRNA is maternal (Fig. 4A,B). Ubiquitous expression was observed during blastula stages and throughout gastrulation (Fig. 4A,C). Shortly after shield formation, weak expression in DFCs emerged (Fig. 4D). Between somite stages 5 and 9, expression in the tailbud and around the KV was detected above the more uniform expression in the embryo (Fig. 4E).

The persistence of LR defects (despite normal gastrulation movements in embryos injected with lower dose of Ttrap[MO]), together with its expression in the KV, suggests that Ttrap is involved in node formation and/or function. However, defective shield formation in Ttrap[MO] embryos also implied that forerunner cell fate could be affected, but DFCs are still present in Ttrap[MO] embryos (see below). In addition, some Ttrap[MO] embryos still have a (less distinct) shield, which may be sufficient to induce DFCs. Since Nodal signaling is important for node function (Essner et al., 2005), we addressed the role of Ttrap by exploiting a special feature of zebrafish: at midblastula transition, the syncytium between yolk and animal cells closes except for cytoplasmic bridges connected to DFCs, the cells that will form KV (Cooper and D'Amico, 1996; Essner et al., 2005). These channels remain open until ~4 hpf. Between 2 and 4 hpf, MO injection results in DFC-specific knockdown (Amack and Yost, 2004); fluorescence-tagged MOs allow for visual control and selection of DFC-specific (DFCMO) injected embryos.

Ttrap[DFCMO] embryos gastrulated normally, yet still displayed randomized heart looping or cardia bifida (48 hpf; Table 4), and again asymmetry markers were missing, expressed bilaterally or unilaterally on the opposite side (Table 5). Analysis of Ttrap[DFCMO] embryos revealed that the KV was either absent or smaller (Fig. 4G), and normal in control[DFCMO] embryos (Fig. 4F), even at 16 ng. We confirmed the KV phenotype using the node marker *chemokine receptor-4* (*cxcr4a*) (Thisse et al., 2001) (Fig. 4H,I). These findings indicate that Ttrap plays a role in establishing LR asymmetry by regulating the formation of KV.

TTRAP complexes with Alk4 and Smad3 but not Smad2 or Smad4

Flag-TTRAP plasmid was co-transfected with plasmids encoding HA-tagged Smad2/3/4 into HEK293T cells, and proteins were immunoprecipitated with anti-Flag antibody, and the precipitates resolved by SDS-PAGE, followed by western blot analysis for HA-Smad. TTRAP associated only with Smad3 (Fig. 5A-C). We also tested co-immunoprecipitation between human TTRAP and mouse Alk4. Myc-Alk4 and Flag-TTRAP were co-produced, precipitated with anti-Flag antibody and the precipitates analyzed via blotting for Myc-Alk4. We observed binding of Alk4 to TTRAP (Fig. 5D). A triple complex between TTRAP, Alk4 and Smad3 was not detected, indicating mutually exclusive association of TTRAP with Alk4 and Smad3 (data not shown).

ALK4 phosphorylates TTRAP

TTRAP could serve as substrate for ALK4 kinase. Purified TTRAP was incubated with human ALK4 and the reaction product analyzed by SDS-PAGE followed by autoradiography. ALK4 phosphorylated TTRAP in vitro (Fig. 6A). The band migrating at the position of TTRAP was excised and analyzed by LC-MS/MS. One TTRAP peptide was phosphorylated either on T88 and T92, or on T92 only (Fig. 6B). T88 in TTRAP is highly conserved across species,
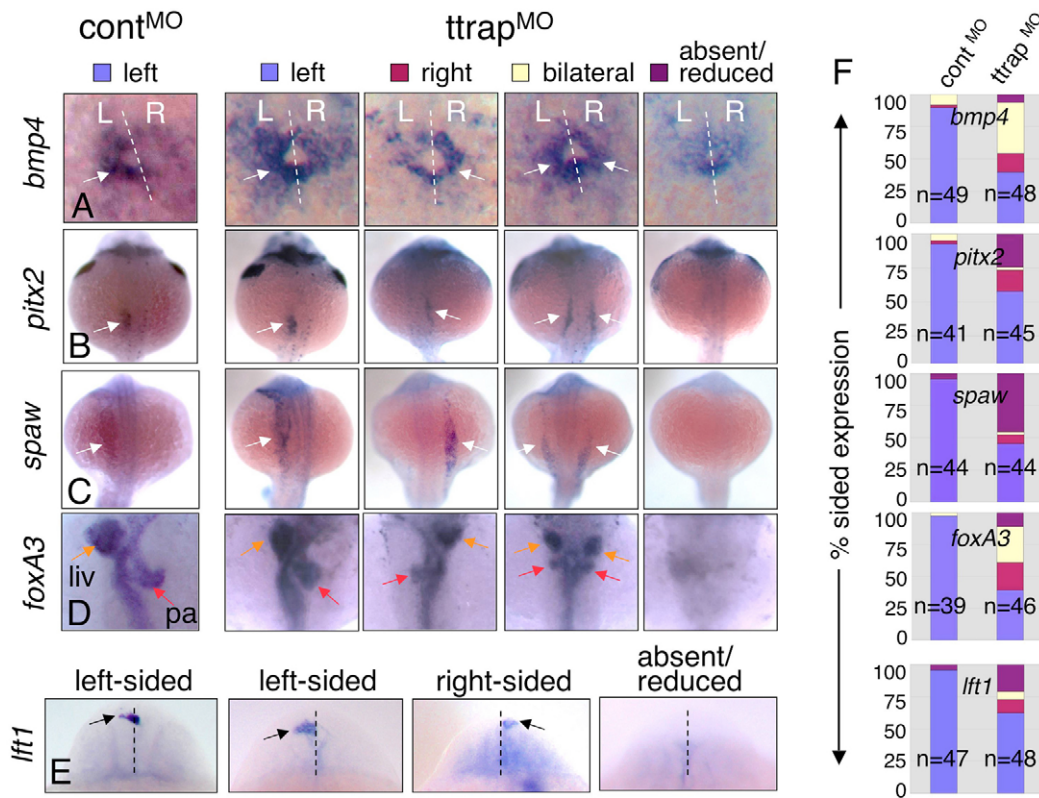
Fig. 3. Randomized LR gene expression and organ laterality in Ttrap^MO embryos. (A-E) Left-sided, right-sided, bilateral or absent/reduced marker expression. For all panels, dorsal views, anterior at top; single arrows denote sidedness, double arrows bilateral expression. (A) *bmp4* in cardiac primordium (22 ss). Dashed white line denotes midline (L, left; R, right). (B,C) *pitx2* and *spaw* in LPM (22 ss). (D) *foxA3*, 48 hpf (orange arrow, liver, liv; red arrow, pancreas, pa). (E) *lft1* in the diencephalon (22-24 ss). Dashed line indicates midline; arrows indicate the relevant altered expression domain. (**F**) Bar graphs showing percentage of embryos with sided expression of these markers within each phenotypic category (*y*-axis), in control^MO and Ttrap^MO embryos (*x*-axis). Blue bars, left-sided expression; red, right-sided; yellow, bilateral; purple, absent/reduced expression. *n*=total embryos from two experiments.

whereas T92 is exclusive to human, dog and chicken (see Fig. S2 in the supplementary material). We tested in vivo phosphorylation of Strep-TTRAP by co-expression with mouse Alk4 in HEK293T cells, and affinity-purified TTRAP. In this preparation TTRAP-specific peptides were reproducibly found in both the singly (T92) and doubly phosphorylated form (T88/T92) (not shown).

We then mutagenized TTRAP by substituting Thr88 and Thr92. TTRAP^{T88A,T92A} was still capable of associating with Smad3 (see Fig. S3 in the supplementary material) and we therefore tested this mutant in vivo. As mentioned previously, huTTRAP mRNA can partially rescue the Ttrap^MO phenotype (see Table S4 in the

supplementary material) and therefore huTTRAP can substitute for zfTtrap. TTRAP^{T88A,T92A}-RNA-injected embryos were completely normal (Fig. 6C) despite detection of TTRAP^{T88A,T92A} protein in these embryos between 2 and 6 hours after injection at levels similar to wild-type TTRAP (see Fig. S3 in the supplementary material). To rule out the possibility that endogenous Ttrap was somehow rescuing any potential effect(s) of TTRAP^{T88A,T92A}, we co-injected TtrapMO with TTRAP^{T88A,T92A} RNA. This yielded a similar penetrance of gastrulation defects (absence of shield and thickened germ ring) in embryos injected with TtrapMO alone (35%, *n*=40 for TtrapMO+TTRAP^{T88A,T92A} mRNA (300 pg) versus 38% (*n*=42) for

Table 3. Ttrap knockdown randomizes LR gene expression and organ laterality

ISH marker	Stage	Morpholino	Dose	Total *n*	Left	Right	Bilateral	Strongly reduced	χ^2	$P\leq$
bmp4	22 ss	Control MO	4 ng	49	90%	2%	8%	0%	26.8	0.001
		Ttrap MO	4 ng	48	40%	15%	40%	6%		
pitx2	22 ss	Control MO	4 ng	41	93%	2%	5%	0%	13.7	0.001
		Ttrap MO	4 ng	45	58%	16%	2%	24%		
spaw	22 ss	Control MO	4 ng	44	95%	0%	0%	5%	26.4	0.001
		Ttrap MO	4 ng	44	45%	7%	2%	45%		
foxA3	48 hpf	Control MO	4 ng	39	97%	0%	3%	0%	31.9	0.001
		Ttrap MO	4 ng	46	39%	22%	28%	11%		
lft1	22 ss	Control MO	4 ng	47	96%	0%	0%	4%	15.8	0.001
		Ttrap MO	4 ng	48	63%	10%	0%	21%		

ss, somite stage; *pitx2*, *bmp4* and *spaw* were used as markers for the left lateral plate mesoderm. *foxA3* was used as a marker for the liver, pancreas and gut. *lft1* was used as a marker for the left dorsal diencephalon. Data are combined from two separate experiments. Chi-square analysis: Ttrap^MO vs control^MO; total no. of normal embryos vs total no. of embryos with LR defects.
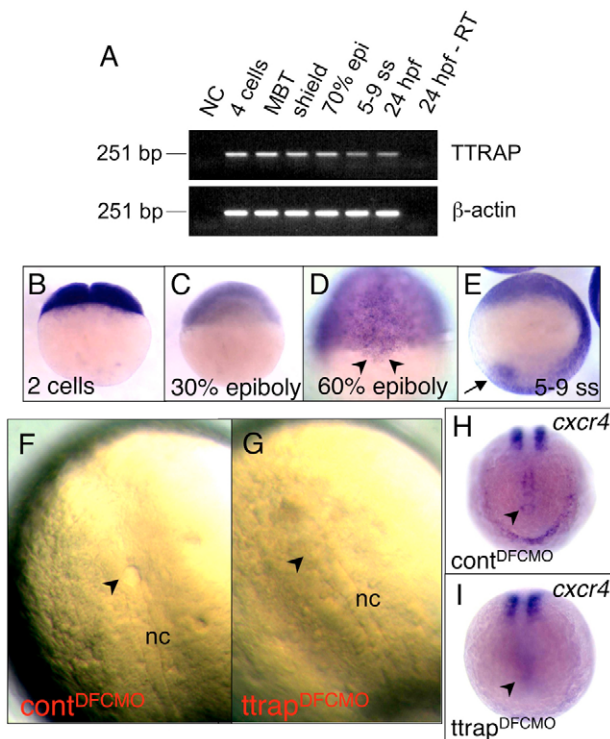
Fig. 4. Expression of *ttrap* and its role during Kupffer's vesicle formation. (**A**) Transcripts are detectable by RT-PCR throughout the first 24 hpf (MBT, mid-blastula transition; epi, epiboly; ss, somite stage). β-actin sequences are shown as loading control (NC, negative control; –RT, no reverse transcriptase). (**B-E**) Whole-mount ISH (WISH) analysis of *ttrap*. (B) Maternal *ttrap* mRNA contribution during early cleavage stages. (C) At 30% epiboly, transcripts are distributed throughout the blastula. Lateral views, animal pole at top. (D) At 60% epiboly, expression in DFCs becomes detectable (arrowheads). Dorsal view, animal pole at top. (E) In addition to the uniform expression throughout the embryo, stronger expression within tailbud and surrounding Kupffer's vesicle (KV, arrow) from 5 ss was observed. (**F-I**) Absence of KV in Ttrap[DFCMO] embryos. (F) KV is present in control[DFCMO] embryo and not detectable in (G) Ttrap[DFCMO] embryo (16 ng MO; arrowheads, KV). Embryos scored live (5-9ss). Posterior views; nc, notochord. (H,I) WISH for *cxcr4a* (5-9 ss) to confirm KV in (H) control[DFCMO] embryo and (I) absence in Ttrap[DFCMO] (arrowheads). Posterior views.

TtrapMO only; Fig. 6C,D, and not shown). Thus, mutant TTRAP[T88A,T92A] is not able to rescue the TtrapMO phenotype, suggesting that phosphorylation of Ttrap on Thr88 and Thr92 is essential for Ttrap function.

Ttrap limits Smad3 activity during zebrafish development

The results of the co-immunoprecipitation (Fig. 5) suggest a role for Ttrap in modulating Alk4/Smad3 signaling. To test whether binding of TTRAP to Smad3 directly modulates Smad3 activity, we performed reporter assays using a Smad2/3-responsive element in vivo. ARE-luciferase reporter (Yeo et al., 1999) (or pGL3 as negative control) was co-injected with Ttrap[MO] into embryos, and luciferase measured in lysates from pooled embryos at shield stage. Co-injection resulted in ~fivefold higher Smad2/3 activity over control[MO] (mean value 4.6±2.5, $P \leq 0.01$; Student's unpaired *t*-test) (Fig. 7A). To test whether this increase is dependent on Nodal signaling, we repeated the assay in the presence of Sqt or Cyc. The addition (via RNA injection) of either ligand to Ttrap[MO] embryos potentiated ARE-luciferase tenfold above the activity detected with Sqt (or Cyc) but without Ttrap[MO] (Fig. 7B). Thus, Ttrap appears to negatively modulate Nodal signaling in vivo.

We also tested whether expression of Smad3 targets was misregulated in Ttrap[MO] embryos. In contrast to Smad2, there is a striking paucity for known Smad3 targets with regard to Nodal/Alk4 signaling. In *Xenopus*, one reported target of both Smad2 and Smad3 is *Mix-2* (Yeo et al., 1999). The fish mutant *bon* harbors a mutation in the *mixer-like* gene and displays cardia bifida (Chen et al., 1996; Stainier et al., 1996; Kikuchi et al., 2000). The characterization of the *bon* promoter and its activation by Smad2/3 has not been reported. We observed an increase in *bon* staining in Ttrap[MO] embryos (Fig. 7C,D). We also tested whether Smad3 RNA injection would upregulate *bon*. In zebrafish two *smad3* genes exist, *smad3a* (Dick et al., 2000) and *smad3b* (Pogoda and Meyer, 2002). Because a gastrulation phenotype has been reported for Smad3b RNA-injected embryos and *smad3b* is expressed in the tailbud region (i.e. in the vicinity of KV), we focused on *smad3b*. Importantly, Smad2 overproduction does not result in gastrulation defects (Muller et al., 1999; Dick et al., 2000). In embryos overexpressing Smad3b (Smad3b[OE]), endogenous *bon* was strongly upregulated (Fig. 7E,F; and data not shown).

To determine whether modulation of Smad3 activity by Ttrap depends on Alk4 signaling, we soaked embryos from dome stage onwards in the Alk4/5/7 inhibitor SB431542 (Inman et al., 2002), 50 μM of which phenocopied the *cyc;sqt* double mutant by shield stage (Feldman et al., 1998) (not shown) and abolished *bon* expression in Ttrap[MO] embryos (Fig. 7G,H). Thus, the upregulation of *bon* in Ttrap[MO] embryos appears to depend on Alk signaling. Ttrap mRNA levels are not affected by SB431542 (not shown). Morphological observation of live Smad3b[OE] embryos and WISH for *papc* and *myod* revealed CE and epiboly defects similar to Ttrap[MO] embryos (Fig. 7L-N). In addition, overexpression of Smad3b in DFCs also induced a low percentage of heart-looping defects (see Table S5 in the supplementary material). Since targeting of mRNA to DFCs has not been previously reported, we initially determined whether DFC-specific expression could be achieved, using eGFP RNA. Fluorescence was detectable in the node at the time of KV formation, and all embryos developed normally. However, in the majority of embryos, only part of the KV was fluorescent, indicating that not all DFCs were targeted or expressed eGFP. Therefore, DFC-RNA overexpression may not be as efficient as DFC-MO injections (see Fig. S4 in the supplementary material). Nevertheless, about 20% of DFC-Smad3b mRNA-injected embryos displayed heart-looping defects.

Table 4. DFC-specific ttrap knockdown randomizes direction of heart looping

ISH marker	Stage	Morpholino	Dose	Total n	Normal	Reverse	No looping	Cardia bifida	Rudiments*	χ^2	$P \geqslant$
cmlc2	48 hpf	Control DFCMO	16 ng	166	99%	0%	1%	0%	0%	156	0.001
		Ttrap DFCMO	16 ng	259	39%	5%	21%	26%	8%		

*These defects precluded ability to score for direction of heart looping. Data are combined from four separate experiments. Chi-square analysis: TtrapDFCMO vs controlDFCMO; total no. of normal embryos vs total no. of embryos with looping defects.

Table 5. DFC-specific Ttrap knockdown randomizes LR gene expression and organ laterality

ISH marker	Stage	Morpholino	Dose	Total n	Left	Right	Bilateral	Strongly reduced	χ^2	$P \leq$
bmp4	22 ss	Control DFCMO	16 ng	69	91%	7%	1%	0%	28.7	0.001
		Ttrap DFCMO	16 ng	58	48%	12%	38%	2%		
pitx2	22 ss	Control DFCMO	16 ng	45	96%	0%	2%	2%	19.4	0.001
		Ttrap DFCMO	16 ng	69	58%	10%	20%	12%		
spaw	22 ss	Control DFCMO	16 ng	60	85%	5%	0%	10%	35.4	0.001
		Ttrap DFCMO	16 ng	74	34%	27%	24%	15%		
foxA3	48 hpf	Control DFCMO	16 ng	56	100%	0%	0%	0%	23.9	0.001
		Ttrap DFCMO	16 ng	84	63%	6%	10%	21%		
lft1	22 ss	Control DFCMO	16 ng	n.d.	n.d.	n.d.	n.d.	n.d.	n/a	n/a
		Ttrap DFCMO	16 ng	n.d.	n.d.	n.d.	n.d.	n.d.		

*These defects precluded ability to score for direction of heart looping. n.d., not determined; n/a, not applicable. Data are combined from two separate experiments. Chi-square analysis: TtrapDFCMO vs controlDFCMO; total no. of normal embryos vs total no. of embryos with LR defects.

If Ttrap knockdown increases Smad3 activity, then simultaneous reduction of Smad3 in Ttrap[MO] embryos should rescue the Ttrap knockdown phenotype. Indeed, graded double knockdowns of Ttrap-Smad3b rescued up to 70% of Ttrap[MO] embryos with gastrulation and node formation defects (Fig. 8A-C and Tables S6-S8 in the supplementary material). Consistent with our co-immunoprecipitation data, Ttrap-Smad2 double knockdowns did not rescue gastrulation defects in Ttrap[MO] embryos (see Table S9 in the supplementary material). Single Smad2 knockdown resulted in a curved, shortened body axis, anterior truncation, and loss of floorplate (see Fig. S5 in the supplementary material), reminiscent of mutant *sur* (Pogoda et al., 2000; Sirotkin et al., 2000) and similar to the phenotype described for Smad2 knockdown in *Xenopus* (Rana et al., 2006).

Nodal regulates its own expression and that of its antagonists (Bisgrove et al., 1999; Meno et al., 1999; Cheng et al., 2000; Feldman et al., 2002). We tested whether Ttrap knockdown would

alter expression of *cyc*, *sqt* (Rebagliati et al., 1998a; Rebagliati et al., 1998b) and *lft1*. Ttrap was neither required for initiation nor maintenance of *cyc*, *sqt* and *lft1* expression at germ ring stage and 70% epiboly (not shown). This is consistent with our data showing no detectable interaction between TTRAP and Smad2, since expression of *cyc*, *sqt* and *lft1* is regulated primarily by Smad2/FoxHI (Schier, 2003). Ttrap may therefore play a role in distinguishing between Smad2 and Smad3 signaling.
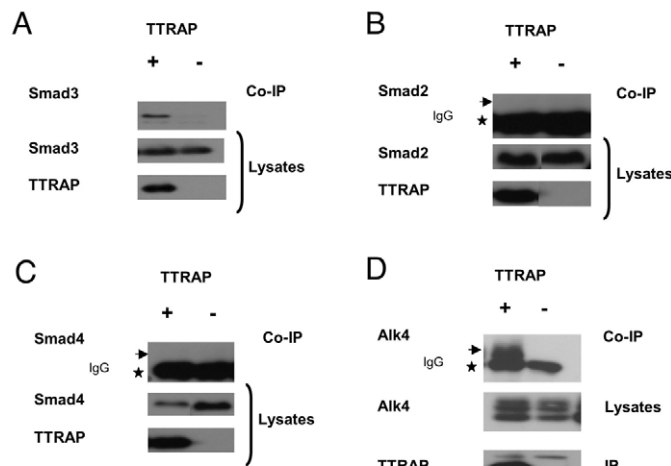
Fig. 6. ALK4 phosphorylates TTRAP. (**A**) SDS-PAGE showing in vitro phosphorylation of TTRAP (arrowhead) and ALK4 autophosphorylation (arrow), when incubated with [γ-^{32}P]ATP and ALK4 kinase (+; – denotes no ALK4 added). (**B**) LC-MS/MS plot depicting in vitro phosphopeptides with T88(phos) and T92(phos). (**C,D**) Phospho-T88 and phospho-T92 are essential for Ttrap function. (C) mRNA injection, yielding overproduction of TTRAP[T88A/T92A], is compatible with normal gastrulation. Live embryo at 80% epiboly showing normal germ ring (gr) and emerging dorsal axial structures (arrowhead). (D) Injection of TTRAP[T88A/T92A] is incapable of rescuing Ttrap[MO] defects, as evidenced by thickened germ ring and lack of shield/axial structures. These embryos showed a severe delay in epiboly and appeared as if they had not passed germ ring stage even at 8 hpf (normally 80% epiboly). The defects observed in Ttrap[MO] embryos were indistinguishable from Ttrap[MO]+TTRAP[T88A/T92A]-injected embryos (not shown). Animal views, dorsal to the right.

Fig. 5. Ttrap associates with Smad3 and Alk4 in mammalian cells. (**A-C**) Co-immunoprecipitation of TTRAP with Smad3 but not Smad2/4. HA-tagged mouse Smad2, -3 or -4 were co-produced with Flag-TTRAP (+), or Flag-TTRAP-frameshift as control (–), in HEK293T cells and precipitated using anti-Flag antibody. Precipitates were immunoblotted and co-precipitated proteins detected with anti-Smad3 or anti-HA antibody for Smad2 or Smad4. Star indicates IgG and arrow shows lack of co-immunoprecipitation with Smad2/4. (**D**) TTRAP-Alk4 interaction. Myc-Alk4 and Flag-TTRAP (+) or control (–) were co-produced and precipitated using anti-Flag antibody. Precipitates were analyzed with anti-Myc antibody (top panel). Star, IgG; arrow, co-immunoprecipitation of Alk4.
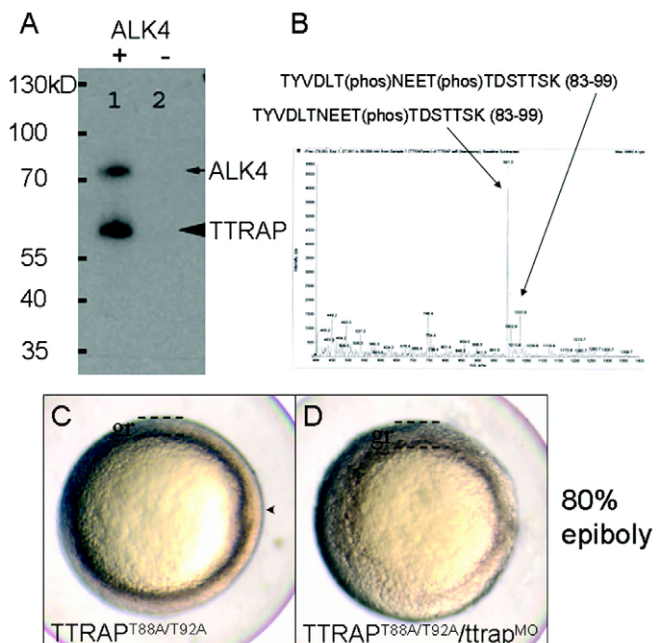
Fig. 7. Ttrap knockdown modulates Nodal-Alk4 signaling. (**A**) Ttrap knockdown increases activity of ARE-luciferase reporter. ARE-lux plasmid (50 pg) was co-injected with Ttrap[MO] (or control[MO]) and embryo lysates assayed for luciferase at shield stage. Knockdown results in ~fivefold greater induction relative to control (4.6±2.5; $P \leq 0.01$; Student's unpaired t-test; eight independent experiments). No significant increase in luciferase was detectable for control pGL3. (**B**) Ttrap[MO] potentiates ARE-lux by sqt or cyc. This experiment was performed as described in A, this time in combination with sqt or cyc mRNA injection (11 pg). The addition of Ttrap[MO] induced ARE-lux an additional tenfold relative to induction by either one of the ligands [81.0±15.6 (ARE+sqt+Ttrap[MO]) vs 9.0±2.6 (ARE+sqt); 38.0±8.6 (ARE+cyc+Ttrap[MO]) vs 3.8±0.8 (are+cyc); $P \leq 0.0001$, One-way analysis of variance (ANOVA)]. y-axis, fold-induction of luciferase. (**C-F**) bon is visibly upregulated in Ttrap[MO] and Smad3b[OE] embryos; WISH at 50% epiboly, animal views (asterisks). (**G,H**) Ttrap[MO]-mediated increase in bon

expression depends on intact alk4 activity. (G) Ttrap[MO] embryo shows strong expression of bon, whereas (H) Ttrap[MO] embryo treated with SB431542 no longer expresses bon. Animal views (asterisks). (**I-N**) Overexpression of Smad3b causes CE and epiboly defects. WISH at 90% epiboly, paraxial mesoderm marker expression in βgal[OE] (700 pg) and Smad3b[OE] (700 pg) embryos. Dorsal-posterior views, anterior at top. (I,L) $papc$ cells fail to converge near the midline in Smad3b[OE] embryos compared with control βgal[OE] embryos. Arrowheads indicate blastopore opening, which is wider in Smad3b[OE] embryos. (J,M) Distance between $myod$ cells is greater in Smad3b[OE] relative to control embryos (double-headed arrows). (K,N) Live observation of β-gal[OE] and Smad3b[OE] embryos, 90% epiboly. (K) Control β-gal[OE] embryo displaying normal epiboly and nearing blastopore closure. (N) Smad3b[OE] embryo showing severe delay in epiboly. Red arrowheads, edge of blastoderm margin. Lateral views, anterior at top. Note that the gastrulation defects depicted here are at an earlier timepoint than those shown for Ttrap[MO] embryos (see Fig. 2). Importantly however, the same gastrulation defects were also observed for Ttrap[MO] embryos at this earlier stage (i.e. 90% epiboly).
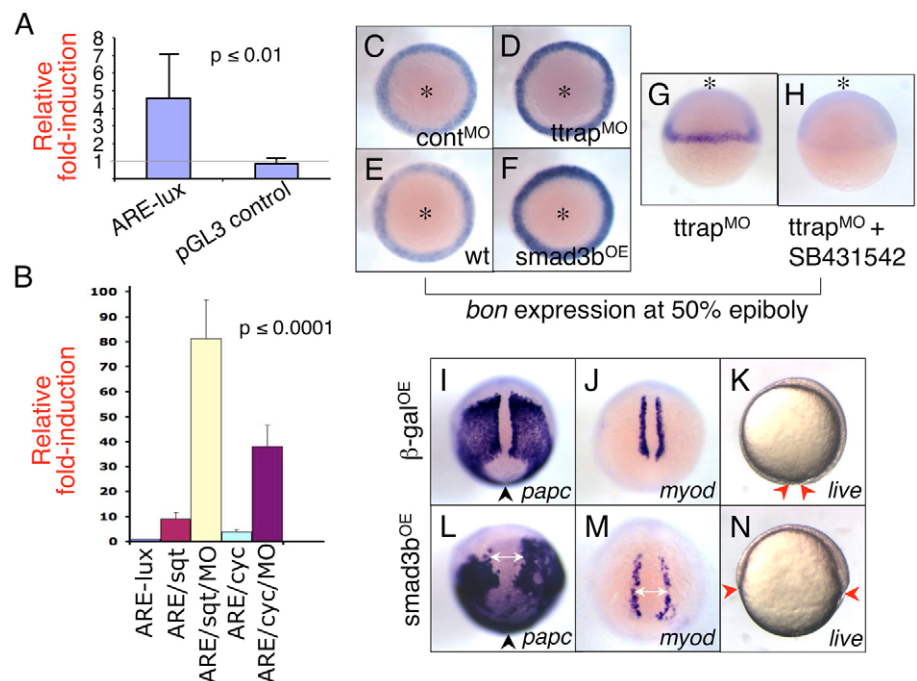
To test whether Ttrap regulation of gastrulation movements is due to a direct effect on cell motility or perturbation of mesendodermal cell fate, we transplanted wild-type and Ttrap[MO] cells sequentially from the lateral margin into the germ ring of *maternal-zygotic one-eyed pinhead* (*MZoep*) embryos (see Fig. S7 in the supplementary material) (Schier et al., 1997; Zhang et al., 1998; Gritsman et al., 1999). In contrast to wild-type cells, Ttrap[MO] cells neither internalized nor migrated to regions normally occupied by endodermal progenitors (as observed for wild-type cells that continue to express *axial* in *MZoep* mutants) (Gritsman et al., 1999). Thus, it appears that Ttrap function (at least its modulation of Smad3 activity) is non cell-autonomous in this context. Moreover, *MZoep* mutants are not rescued by Ttrap knockdown (not shown). This implies that Ttrap knockdown cannot compensate for the lack of Smad2 activation in this Nodal-insensitive *oep* background. This, and our reporter studies, supports our hypothesis that the Ttrap-mediated increase in Smad3 activity is Nodal dependent. In addition, the cell transplantation data implicate a role for Smad3 in specific aspects of Nodal signaling.

Alk4-Ttrap-Smad3 signaling regulates gastrulation and node formation via *cdh1*

Common candidate target genes of Ttrap and Smad3 would help to explain the gastrulation and/or node formation defects in Ttrap[MO] embryos. *cdh1* posed as candidate because the *cdh1* mutant *half-baked* (*hab*) displays epiboly and CE defects similar to Ttrap[MO] embryos, and *cdh1* is expressed in DFCs (Kane et al., 2005; Shimizu et al., 2005).

Because *hab*:*cdh1* null mutants do not survive beyond gastrulation, we again exploited DFC-specific knockdown to determine whether *cdh1* plays a role in node formation. We found randomized heart looping, cardia bifida and smaller/absent KV in cdh1[DFCMO] embryos (Table 6). Analysis of DFCs using *cas/sox32* (Dickmeis et al., 2001; Kikuchi et al., 2001) and prior to node formation revealed that DFCs are present in Ttrap[DFCMO] embryos (Fig. 9A,B). Moreover, at shield and 70-80% epiboly stages, no significant difference in DFC number between Ttrap[MO] and control[MO] embryos was detected (see Fig. S8, Table S10 and Fig. S9 in the supplementary material). However, Ttrap[MO] DFCs do not always converge at the midline to form one tight cluster of cells below the shield or later in gastrulation. Rather, cells are more widely dispersed in a broad stripe along the lateral axis of the embryo (Fig. 9B; see Fig. S8, Table S11, and Fig. S10 in the supplementary material), suggesting a defect in cell migration. In line with our DFC data in Ttrap[MO] embryos, DFCs are still present in *hab*:*cdh1* mutants (Kane et al., 2005). The same DFC defect was also observed in Smad3b[OE] embryos (Fig. 9D) and may reflect an inability of these cells to organize into KV.

We tested whether the DFC defects were due to loss/reduction in *cdh1* in Ttrap[MO] and Smad3b[OE] embryos. At 70% ebiboly (Fig. 9E-H), *cdh1* mRNA (as assessed in these deliberately overstained embryos) was absent in DFCs and the anterior axial hypoblast in both cases (Fig. 9F,H). No significant difference in expression within the epiblast could be detected based on macroscopic observation, but qRT-PCR analysis revealed an overall reduction (30%) of *cdh1* transcript levels in Ttrap[MO] embryos [1.60±0.59,
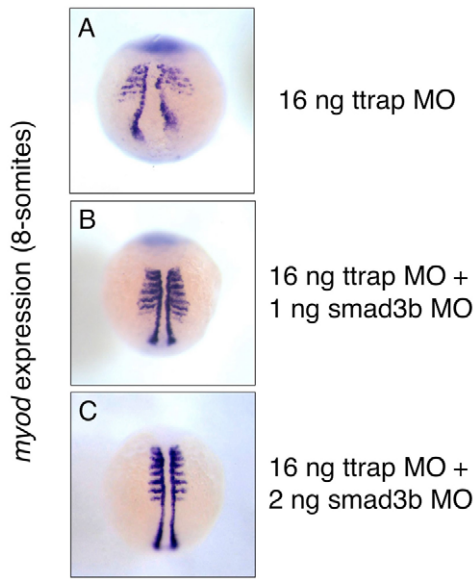
myod expression (8-somites)

16 ng ttrap MO

16 ng ttrap MO +
1 ng smad3b MO

16 ng ttrap MO +
2 ng smad3b MO

Fig. 8. Double Ttrap and Smad3b knockdown rescues CE defect in Ttrap knockdown. *myod* marks paraxial/adaxial mesoderm (8 ss). (**A**) Broadened somites and a wide distance between *myod* cells in Ttrap single knockdown embryo. (**B**) A combination of 16 ng Ttrap[MO] and 1 ng Smad3b[MO] shows closer convergence of *myod* cells at midline. However, somitic expression is still broad relative to the fully rescued embryo co-injected with 2 ng Smad3b[MO] (**C**), which now displays the normal *myod* domain. Dorsal views, anterior at top.

n=30 (Ttrap[MO]) vs 2.3±0.13, *n*=15 (control[MO]); $P \leq 0.01$, Student's unpaired *t*-test; not shown). This limited but consistent reduction may be explained by a Ttrap-Smad3-mediated downregulation of *cdh1* that is localized only to regions where Nodal signaling is present and/or can be sensed, and may therefore be partly masked by more general expression in the rest of the blastoderm.

Ttrap and Smad3 cooperate in the downregulation of *e-cadherin* via upregulation of *snail1a*

Sequence alignment of *e-cadherin* promoters (not shown) revealed no conserved Smad3 sites, making it unlikely that *e-cadherin* downregulation occurs via direct binding of Smad3. One E-box containing the Snail-binding sequence CACC was strictly conserved between human, mouse and zebrafish. Several repressors including Snail bind within E-box elements and inhibit *e-cadherin* expression (Cano et al., 2000; Grooteclaes and Frisch, 2000; Comijn et al., 2001; Hajra et al., 2002; Eger et al., 2000), and *Snail* is induced by TGFβ or Nodal (Fujimoto et al., 2001; Hajra et al., 2002; Peinado et al., 2003; Gotzmann et al., 2006; Bennett et al., 2007).

At 60% epiboly, *snail1a* (*snai1a*) expression is restricted to the blastoderm margin and presumptive paraxial mesoderm, but is excluded from the dorsal most region of the shield (presumptive
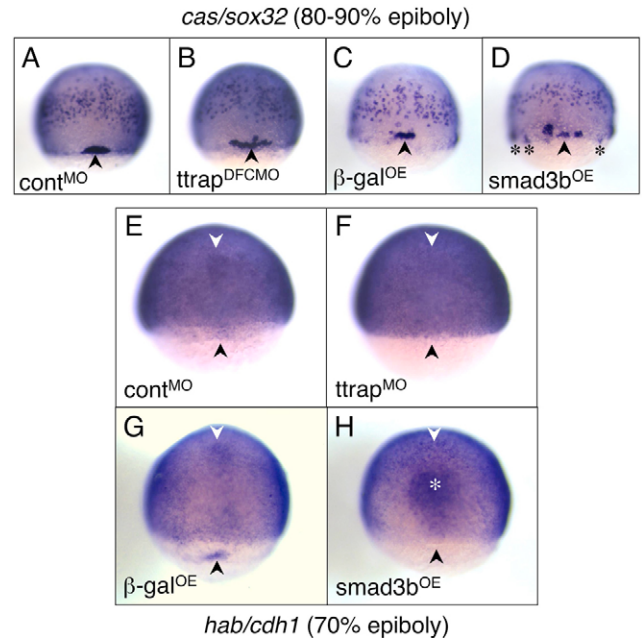
cas/sox32 (80-90% epiboly)

hab/cdh1 (70% epiboly)

Fig. 9. Aberrant DFC migration and clustering as a result of Ttrap-Smad3-mediated downregulation of *cdh1*. (**A-D**) *cas/sox32* as DFC marker, 80-90% epiboly. (A,C) Tight clustering of DFCs (black arrowheads) in control[MO] and βgal[OE] embryos. (B,D) In Ttrap[MO] and Smad3b[OE] embryos, DFCs are more spread out. Occasionally, DFCs are also ectopically located around and just underneath the blastoderm margin (black asterisks). (**E-H**) *cdh1* is absent in DFCs and anterior axial hypoblast of Ttrap[MO] and Smad3b[OE] embryos, 70% epiboly. General *cdh1* expression in the epiblast remains unaltered in all embryos; the embryos are deliberately overstained. (E,G) *cdh1* in DFCs (black arrowheads) and anterior axial hypoblast (white arrowheads) visible in control[MO] and βgal[OE] embryos and missing in (F) Ttrap[MO] and (H) Smad3b[OE] embryos. In Smad3b[OE] embryos, stronger staining in the prechordal plate (white asterisk) was also observed and may be a consequence of a thickening of this region because of hyperdorsalization. Dorsal views, anterior at top.

axial mesoderm) (Hammerschmidt and Nüsslein-Volhard, 1993; Thisse et al., 2001). DFCs are in close proximity to these dorsal cells and do not express *snai1a*. We questioned whether the increase in Smad3 activity in Ttrap[MO] embryos would be sufficient to cause ectopic expression of *snai1a* in either axial mesoderm and/or DFCs, thereby contributing to *cdh1* downregulation. Knockdown of Ttrap resulted in misexpression of *snai1a* in axial mesoderm (60% epiboly; Fig. 10A,B) and DFCs (not shown). To determine whether this expression is mediated by Smad3, we performed Ttrap-Smad3 double knockdowns to test for reversion to the normal *snai1a* domain. Double knockdown resulted in a 58% rescue of embryos with ectopic *snai1a* in the axial mesoderm (Fig. 10C,D; Fig. 10E for

Table 6. DFC-specific Cadherin1 knockdown randomizes direction of heart looping

Assay	Stage	RNA	Dose	Total *n*	Normal	Reverse	No Looping	Cardia bifida	Rudiments*	χ^2	$P\leq$
live	48 hpf	Std control fluor. DFCMO	4 ng	106	96%	1%	3%	0%	0%	59.0	0.001
		Cdh1 DFCMO	4 ng	125	50%	6%	22%	18%	2%		

*These defects precluded ability to score for direction of heart looping. Data are combined from three separate experiments. Chi-square analysis: Cdh1DFCMO vs control DFCMO; total no. of normal embryos vs. total no. of embryos with looping defects.
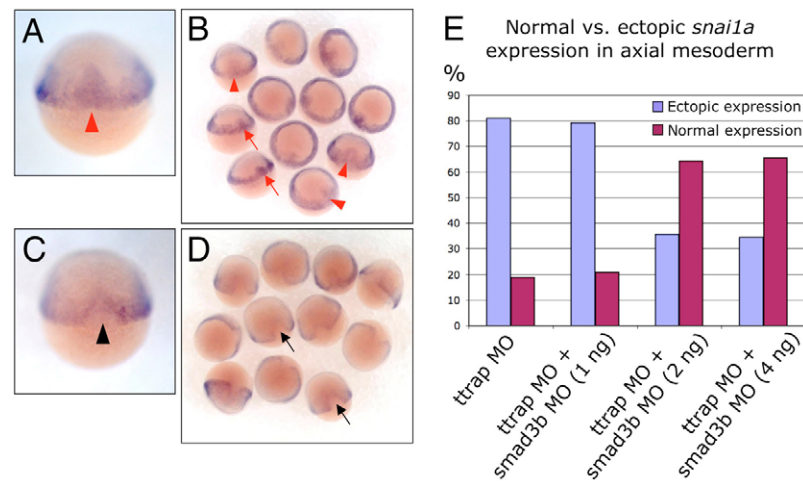
Fig. 10. Knockdown of Ttrap induces ectopic *snai1a* in the shield and DFCs. (**A-D**) WISH for *snai1a*, 60% epiboly. (A,B) *snai1a* transcripts are found in the margin and paraxial mesoderm in Ttrap[MO] embryos, but are also present ectopically in the presumptive axial mesodermal region within the shield (red arrowheads and arrows). (C,D) Rescued Ttrap and Smad3b MO double-knockdown embryos display normal *snai1a* domain, particularly, the exclusion of *snai1a* from the shield (black arrowhead and arrows). Dorsal views, anterior at top. (**E**) Derepression of *snai1a* in axial mesoderm of Ttrap[MO] embryos is mediated by Smad3. Graph depicts partial rescue of Ttrap[MO]-induced *snai1a* phenotype in Ttrap and Smad3 double knockdowns. *y*-axis represents percentage of embryos exhibiting either *snai1a* exclusion from axial mesoderm (purple bars) or ectopic expression in axial mesoderm (blue bars), at 60% epiboly. *x*-axis represents types of MO treatment. 81% of Ttrap[MO] embryos display abnormal *snai1a* domain, whereas simultaneous knockdown of Ttrap and Smad3 reverts up to 58% of these embryos back to the wild-type domain (purple bars).

graphical depiction of rescue; data not shown). Curiously, neither the single Smad3b nor Smad3a knockdown (and their combination) resulted in downregulation of *snai1a* (not shown). Moreover, Smad3b knockdown did not result in any visible gastrulation phenotype/s (our unpublished observations), despite the presence of transcripts throughout early development (Dick et al., 2000; Pogoda and Meyer, 2002). By 24 hpf however, morphological defects similar to the Smad2 knockdown phenotype such as head degeneration, absence of floorplate, and curved, shortened body axis could be observed (see Fig. S6 in the supplementary material). The lack of a phenotype before 24 hpf may be attributed to compensation by either Smad2, Smad3a, and/or Smad2/3 maternal protein/s. Finally, we performed Ttrap-Snail1a double-knockdowns to test for rescue of Ttrap-induced LR defects. This resulted in a 62% rescue of heart looping defects (48 hpf; see Table S12 and Fig. S11 in the supplementary material).

DISCUSSION
Ttrap controls gastrulation movements via modulation of Smad3 activity and *cdh1* expression
Ttrap knockdown perturbs gastrulation movements. TTRAP binds to Alk4 and Smad3, and TTRAP limits Smad3 transcriptional activity. The similarities in CE and epiboly defects between the Ttrap knockdown embryos and *hab*:*cdh1* mutants led us to investigate the link between *ttrap* and *cdh1*. The importance of Cdh1 in controlling CE and epibolic movements during gastrulation is known (Babb and Marrs, 2004; Kane et al., 2005; Shimizu et al., 2005; Ulrich et al., 2005). Our data suggest that: (1) *cdh1* is downstream of Alk4-Smad3 and that *cdh1* expression may, in part, be controlled by Ttrap through attenuation of Smad3 activity; and (2) that knockdown of Ttrap increases Smad3 activity, which in turn downregulates *cdh1*, thereby leading to impaired CE and epiboly. Our results also implicate snail as a potential link between increase in Smad3 activity and downregulation of *cdh1*, possibly via a snail-binding site in the *cdh1* promoter.

Knockdown of Ttrap does not appear to affect mesodermal or endodermal cell fate, because *bon* and *cas* expression persist in mesendoderm and presumptive endoderm, respectively. This observation was also true for meso/endodermal *bhik*, *mix*, *ntl* and *gsc* (not shown), including in Ttrap[MO] embryos with thickened germ ring. We therefore propose that *ttrap* is primarily involved in cell migration in early embryos. The results of the cell transplantations (both with wild-type and with Ttrap[MO] cells) into a defective Nodal signaling background (*MZoep*) indicate a possible distinct function for Smad3 in directing cell movement. TTRAP has been implicated in migration of cancer cells through its interaction with ETS1/2 and FLI1 (Pei et al., 2003). However, knockdown of Ets1 in fish did not yield gastrulation defects (our unpublished observations), and *fli1* expression only begins after gastrulation at 10 hpf (Brown et al., 2000), making *fli1* an unlikely Ttrap target with respect to regulation of CE movements and epiboly.

Potential role of Ttrap in Kupffer's vesicle formation
LR-axis determination in fish (Kramer-Zucker et al., 2005) and mouse, and the resulting laterality of heart and viscera, is initiated in part by the action of monocilia residing within the node. This structure consists of a 'pit' of cells, with each cell protruding one monocilium, which in mouse is posteriorly tilted at an angle of 60° (Nonaka et al., 2005). The first symmetry-breaking event occurs when these monocilia beat in vortical fashion to direct unidirectional fluid flow, resulting in accumulation of proteins left of the node. Physical models that can mimic such flow have shown that even this small difference in Nodal flow is subsequently converted through reaction-diffusion mechanisms involving Nodal/Lefty proteins into a robust asymmetrical target gene expression (Okada et al., 2005; Hirokawa et al., 2006). This results in activation of target genes in the LPM, which endow 'leftness' to this side of the embryo and activate asymmetrical differentiation of organ primordia. However, the mechanism(s) by which these asymmetric signals are translated into morphology is not well understood (Shiratori and Hamada,

2006). Genes expressed specifically in the right LPM also function in LR determination, and other studies have also implicated the intact midline as serving a barrier function between left- and right-sided factors (Roessler and Muenke, 2001; Tabin and Vogan, 2003; Yost, 2003; Raya and Belmonte, 2004; Levin, 2005; Raya and Belmonte, 2006).

Our findings suggest that Ttrap plays a role both in the earliest steps of KV (node) formation and gastrulation. DFC-specific Ttrap knockdown embryos gastrulate normally, yet DFC behavior is abnormal, resulting in a KV that is strongly reduced in size, or absent. The laterality defects observed in Ttrap[DFCMO] embryos are consistent with LR defects obtained after DFC ablation (Essner et al., 2005). Moreover, we provide results implicating *cdh1* as a possible target of Ttrap and Smad3 for regulating gastrulation movements and KV formation. *E-cadherin* (*cdh1*) is an established player in mediating cell (de)adhesion/migration in embryos and invasive tumors. Our results suggest that *cdh1* may play a role in LR-axis determination. It must be noted, however, that neither KV nor LR defects have been described for *cdh1* mutants to date. It therefore remains to be seen what the precise role is for Cdh1 with regard to LR patterning and DFC migration. Our data suggests that Ttrap regulates *cdh1* via Smad3 as opposed to Smad2. This is supported by a recent siRNA study on the epithelial-to-mesenchymal transition (EMT) of proximal-tubule epithelial cells, which showed a Smad3-dependent (and Smad2-independent) downregulation of *cdh1* following stimulation of cells with TGFβ (Phanish et al., 2006).

Ttrap distinctly modulates Smad3 and not Smad2 activity

Smad2 and Smad3 share over 90% identity and a number of overlapping functions, such as the co-regulation of the Nodal targets *bon* and *snail* (Bennett et al., 2007). Although our results indicate that *bon* and *snail* can be regulated by Smad3, our data do not rule out co-regulation by Smad2, and regulation of these genes most likely occurs via cooperation between these two Smads. Nevertheless, there are structural/functional differences between both Smads, several of which appear to distinguish their actions in vitro (Yew et al., 2004; Uemura et al., 2005; Ju et al., 2006) and in vivo (Dunn et al., 2005; Wang et al., 2006). In addition, the ratio of Smad2 versus Smad3 influences their respective roles as effectors (Dunn et al., 2004; Kim et al., 2005). The functional differences between Smad2 and Smad3 may also depend on their ability to associate with various co-factors that mediate distinct responses to TGFβ (Attisano et al., 2001). These co-factors include Fox proteins (Nagarajan and Chen, 2000) or the Smad-interacting protein Smicl, which primarily modulates Smad3 activity during Nodal-dependent induction of *chordin* in the Spemann organizer (Collart et al., 2005). Clearly, additional Smad2- and Smad3-specific targets and co-factors remain to be identified. Ttrap may be one such co-factor in Nodal-Alk4-Smad3 signaling. Intriguingly, the Ttrap knockdown phenotype does not entirely mimic the Nodal overexpression phenotype (Toyama et al., 1995). In the latter study, Nodal mRNA injection into fish embryos resulted in axis duplication and ectopic organizer formation, phenotypes not observed in Ttrap knockdown embryos. Thus, Ttrap knockdown does not result in a general over-activation of Nodal signaling, which would also encompass Smad2 activity .

The role of Ttrap as a co-factor for ETS (Pei et al., 2003) suggests that intranuclear Ttrap may play a similar role with regard to Smad3. This is supported by the finding that Ttrap binds to SUMO proteins, which are implicated in a number of cellular processes including transcription (Hecker et al., 2006). In any case, several lines of

evidence support the hypothesis of Ttrap as modulator of Alk4-dependent Smad3 activity: (1) the association between TTRAP and Smad3 is mutually exclusive with Alk4; (2) the high degree of overlap between Ttrap[MO] and Smad3b[OE] phenotypes; (3) the ARE-luciferase data; and (4) the rescue of the Ttrap knockdown phenotype via Smad3 knockdown. However, the functional mechanism underlying this modulation remains to be investigated in detail.

The roles of Smad2/3 as effectors have been extensively characterized in the mouse, including elegant studies that address the effects of changing their ratio in vivo in Nodal-controlled mesoderm formation (Dunn et al., 2004; Dunn et al., 2005). Our data show that Smad3 plays an important role in zebrafish in controlling cell migration and/or (de)adhesion through Nodal-Alk4. Sqt is the most likely ligand here because of its reported role in regulating gastrulation movements and its expression in DFCs (Rebagliati et al., 1998b; Feldman et al., 2000). Ttrap may serve as limiting factor for Smad3, perhaps to maintain a balance between Smad2 (the DNA-binding splice form) and Smad3 signaling, because both are capable of occupying the same promoter sites of target genes for Nodal.

Using biochemical studies and phenotypic analysis in zebrafish, we have uncovered a role for Ttrap as a novel player in TGFβ signaling in vivo. Our findings suggest that this protein is essential for regulating Nodal signaling, at least by limiting the early developmental activity of Smad3. Given that extranuclear Ttrap and Alk4 also interact either directly or are present together in a complex, it is possible that Alk4 itself, via a negative feedback loop involving Ttrap and possibly other co-factors, functions to regulate the level of its own signal transduction cascade. This type of higher order regulation fits in the concept of self-enabled gene response cascades (Massagué et al., 2005) and has been observed in TGFβ-Smad signaling. Although further studies are needed to elucidate the exact mechanism by which Ttrap modulates Alk4-Smad3 activity, our data underscore the importance of tightly fine-tuning TGFβ-Smad pathways in embryos.

Supplementary material
Supplementary material for this article is available at
http://dev.biologists.org/cgi/content/full/134/24/4381/DC1

References
Alexander, J., Rothenberg, M., Henry, G. L. and Stainier, D. Y. (1999). casanova plays an early and essential role in endoderm formation in zebrafish. *Dev. Biol.* **215**, 343-357.
Amack, J. D. and Yost, H. J. (2004). The T-box transcription factor no tail in ciliated cells controls zebrafish left-right asymmetry. *Curr. Biol.* **14**, 685-690.
Attisano, L., Silvestri, C., Izzi, L. and Labbé, E. (2001). The transcriptional role of Smads and Fast (FoxHI) in TGFβ and activin signalling. *Mol. Cell. Endocrinol.* **180**, 3-11.
Babb, S. G. and Marrs, J. A. (2004). E-cadherin regulates cell movements and tissue formation in early zebrafish embryos. *Dev. Dyn.* **230**, 263-277.
Bennett, J. T., Joubin, K., Cheng, S., Aanstad, P., Herwig, R., Clark, M., Lehrach, H. and Schier, A. F. (2007). Nodal signaling activates differentiation genes during zebrafish gastrulation. *Dev. Biol.* **304**, 525-540.
Bisgrove, B. W., Essner, J. J. and Yost, H. J. (1999). Regulation of midline development by antagonism of lefty and nodal signaling. *Development* **126**, 3253-3262.
Branford, W. W. and Yost, H. J. (2004). Nodal signaling: Cryptic-Lefty mechanism of antagonism decoded. *Curr. Biol.* **14**, 341-343.

Brown, L. A., Rodaway, A. R. F., Schilling, T. F., Jowett, T., Ingham, P. W., Patient, R. K. and Sharrocks, A. D. (2000). Insights into the early vasculogenesis revealed by expression of the ETS-domain transcription factor Fli-1 in wild-type and mutant zebrafish embryos. *Mech. Dev.* **90**, 237-252.

Campione, M., Steinbeisser, H., Schweickert, A., Deissler, K., van Bebber, F., Lowe, L. A., Nowotschin, S., Viebahn, C., Haffter, P., Kuehn, M. R. et al. (1999). The homeobox gene Pitx2: mediator of asymmetric left-right signalling in vertebrate heart and gut looping. *Development* **126**, 1225-1234.

Cano, A., Perez-Moreno, M. A., Rodrigo, I., Locascio, A., Blanco, M. J., del Barrio, M. G., Portillo, F. and Nieto, M. A. (2000). The transcription factor Snail controls epithelial-mesenchymal transitions by repressing E-cadherin expression. *Nat. Cell Biol.* **2**, 76-83.

Chen, J. N., Haffter, P., Odenthal, J., Vogelsang, E., Brand, M., van Eeden, F. J., Furutani-Seiki, M., Granato, M., Hammerschmidt, M., Heisenberg, C. P. et al. (1996). Mutations affecting the cardiovascular system and other internal organs in zebrafish. *Development* **123**, 293-302.

Chen, J. N., van Eeden, F. J., Warren, K. S., Chin, A., Nusslein-Volhard, C., Haffter, P. and Fishman, M. C. (1997). Left-right pattern of cardiac BMP4 may drive asymmetry of the heart in zebrafish. *Development* **124**, 4373-4382.

Cheng, A. M., Thisse, B., Thisse, C. and Wright, C. V. (2000). The lefty-related factor Xatv acts as a feedback inhibitor of nodal signaling in mesoderm induction and L-R axis development in *Xenopus*. *Development* **127**, 1049-1061.

Collart, C., Verschueren, K., Rana, A., Smith, J. C. and Huylebroeck, D. (2005). The novel Smad-interacting protein Smicl regulates Chordin expression in the *Xenopus* embryo. *Development* **132**, 4575-4586.

Comijn, J., Berx, G., Vermassen, P., Verschueren, K., van Grunsven, L., Bruyneel, E., Mareel, M., Huylebroeck, D. and van Roy, F. (2001). The two-handed E box binding zinc finger protein SIP1 downregulates e-cadherin and induces invasion. *Mol. Cell* **7**, 1267-1278.

Cooper, M. S. and D'Amico, L. A. (1996). A cluster of noninvoluting endocytic cells at the margin of the zebrafish blastoderm marks the site of embryonic shield formation. *Dev. Biol.* **180**, 184-198.

Dick, A., Mayr, T., Bauer, H., Meier, A. and Hammerschmidt, M. (2000). Cloning and characterization of zebrafish Smad2, Smad3 and Smad4. *Gene* **246**, 69-80.

Dickmeis, T., Mourrain, P., Saint-Etienne, L., Fischer, N., Aanstad, P., Clark, M., Strahle, U. and Rosa, F. (2001). A crucial component of the endoderm formation pathway, CASANOVA, is encoded by a novel sox-related gene. *Genes Dev.* **15**, 1487-1492.

Dougan, S. T., Warga, R. M., Kane, D. A., Schier, A. F. and Talbot, W. S. (2003). The role of the zebrafish nodal-related genes squint and cyclops in patterning of mesendoderm. *Development* **130**, 1837-1851.

Dunn, N. R., Vincent, S. D., Oxburgh, L., Robertson, E. J. and Bikoff, E. K. (2004). Combinatorial activities of Smad2 and Smad3 regulate mesoderm formation and patterning in the mouse embryo. *Development* **131**, 1717-1728.

Dunn, N. R., Koonce, C. H., Anderson, D. C., Islam, A., Bikoff, E. K. and Robertson, E. J. (2005). Mice exclusively expressing the short isoform of Smad2 develop normally and are viable and fertile. *Genes Dev.* **19**, 152-163.

Eger, A., Stockinger, A., Schaffhauser, B., Beug, H. and Foisner, R. (2000). Epithelial mesenchymal transition by c-Fos estrogen receptor activation involves nuclear translocation of beta-catenin and upregulation of beta-catenin/lymphoid enhancer binding factor-1 transcriptional activity. *J. Cell Biol.* **148**, 173-188.

Essner, J. J., Amack, J. D., Nyholm, M. K., Harris, E. B. and Yost, H. J. (2005). Kupffer's vesicle is a ciliated organ of asymmetry in the zebrafish embryo that initiates left-right development of the brain, heart and gut. *Development* **132**, 1247-1260.

Feldman, B., Gates, M. A., Egan, E. S., Dougan, S. T., Rennebeck, G., Sirotkin, H. I., Schier, A. F. and Talbot, W. S. (1998). Zebrafish organizer development and germ-layer formation require nodal-related signals. *Nature* **395**, 181-185.

Feldman, B., Concha, M. L., Saude, L., Parsons, M. J., Adams, R. J., Wilson, S. W. and Stemple, D. L. (2002). Lefty antagonism of squint is essential for normal gastrulation. *Curr. Biol.* **12**, 2129-2135.

Fujimoto, K., Sheng, H., Shao, J. and Beauchamp, R. D. (2001). Transforming growth factor-β1 promotes invasiveness after cellular transformation with activated Ras in intestinal epithelial cells. *Exp. Cell Res.* **266**, 239-249.

Gotzmann, J., Fischer, A. N. M., Zojer, M., Mikula, M., Proell, V., Huber, H., Jechlinger, M., Waerner, T., Weith, A., Beug, H. et al. (2006). A crucial function of PDGF in TGFβ-mediated cancer progression of hepatocytes. *Oncogene* **25**, 3170-3185.

Gritsman, K., Zhang, J., Cheng, S., Heckscher, E., Talbot, W. S., Schier, A. F. (1999). The EGF-CFC protein one-eyed pinhead is essential for nodal signaling. *Cell* **97**, 121-132.

Grooteclaes, M. L. and Frisch, S. M. (2000). Evidence for a function of CtBP in epithelial gene regulation and anoikis. *Oncogene* **19**, 3823-3828.

Hajra, K. M., Chen, D. Y. and Fearon, E. R. (2002). The SLUG zinc-finger protein represses E-cadherin in breast cancer. *Cancer Res.* **62**, 1613-1618.

Hammerschmidt, M. and Nüsslein-Volhard, C. (1993). The expression of a zebrafish gene homologous to *Drosophila* snail suggests a conserved function in invertebrate and vertebrate gastrulation. *Development* **119**, 1107-1118.

Hauptmann, G. and Gerster, T. (1994). Two-color whole-mount in situ hybridization to vertebrate and *Drosophila* embryos. *Trends Genet.* **10**, 266.

Hecker, C. M., Rabiller, M., Haglund, K., Bayer, P. and Dikic, I. (2006). Specification of SUMO1- and SUMO2-interacting motifs. *J. Biol. Chem.* **281**, 16117-16127.

Hill, C. S. (2001). TGFβ signaling pathways in early *Xenopus* development. *Curr. Opin. Genet. Dev.* **11**, 533-540.

Hirokawa, N., Tanaka, Y., Okada, Y. and Takeda, S. (2006). Nodal flow and the generation of left-right asymmetry. *Cell* **125**, 33-45.

Inman, G. J., Nicolas, F. J., Callahan, J. F., Harling, J. D., Gaster, L. M., Reith, A. D., Laping, N. J. and Hill, C. S. (2002). SB-431542 is a potent and specific inhibitor of transforming growth factor-beta superfamily type I activin receptor-like kinase (ALK) receptors ALK4, ALK5 and ALK7. *Mol. Pharmacol.* **62**, 65-74.

Ju, W., Ogawa, A., Heyer, J., Nierhof, D., Yu, L., Kucherlapati, R., Shafritz, D. A. and Bottinger, E. P. (2006). Deletion of Smad2 in mouse liver reveals novel functions in hepatocyte growth and differentiation. *Mol. Cell. Biol.* **26**, 654-667.

Kane, D. A., McFarland, K. N. and Warga, R. M. (2005). Mutations in half-baked/e-cadherin block cell behaviors that are necessary for teleost epiboly. *Development* **132**, 1105-1116.

Kikuchi, Y., Trinh, L. A., Reiter, J. F., Alexander, J., Yelon, D. and Stainier, D. Y. (2000). The zebrafish *bonnie and clyde* gene encodes a Mix family homeodomain protein that regulates the generation of endodermal precursors. *Genes Dev.* **14**, 1279-1289.

Kikuchi, Y., Agathon, A., Alexander, J., Thisse, C., Waldron, S., Yelon, D., Thisse, B. and Stainier, D. Y. (2001). Casanova encodes a novel Sox-related protein necessary and sufficient for early endoderm formation in zebrafish. *Genes Dev.* **15**, 1493-1505.

Kim, S. G., Kim, H. A., Jong, H. S., Park, J. H., Kim, N. K., Hong, S. H., Kim, T. Y. and Bang, Y. J. (2005). The endogenous ratio of Smad2 and Smad3 influences the cytostatic function of Smad3. *Mol. Biol. Cell* **16**, 4672-4683.

Kishigami, S. and Mishina, Y. (2005). BMP signaling and early embryonic patterning. *Cytokine Growth Factor Rev.* **16**, 265-278.

Kramer-Zucker, A. G., Olale, F., Haycraft, C. J., Yoder, B. K., Schier, A. F. and Drummond, I. A. (2005). Cilia-driven fluid flow in the zebrafish pronephros, brain and Kupffer's vesicle is required for normal organogenesis. *Development* **132**, 1907-1921.

Kunwar, P. S., Zimmerman, S., Bennett, J. T., Chen, Y., Whitman, M. and Schier, A. F. (2003). Mixer/Bon and FoxHl/Sur have overlapping and divergent roles in Nodal signaling and mesendoderm induction. *Development* **130**, 5589-5599.

Lawson, N. D. and Weinstein, B. M. (2002). In vivo imaging of embryonic vascular developmentusing transgenic zebrafish. *Dev. Biol.* **248**, 307-318.

Levin, M. (2005). Left-right asymmetry in embryonic development: a comprehensive review. *Mech. Dev.* **122**, 3-25.

Liang, J. O., Etheridge, A., Hantsoo, L., Rubinstein, A. L., Nowak, S. J., Izpisúa Belmonte, J. C. and Halpern, M. E. (2000). Asymmteric Nodal signaling in the zebrafish diencephalon positions the pineal organ. *Development* **127**, 5101-5112.

Liao, W., Bisgrove, B. W., Sawyer, H., Hug, B., Bell, B., Peters, K., Grunwald, D. J. and Stainier, D. Y. (1997). The zebrafish gene cloche acts upstream of a flk-1 homologue to regulate endothelial cell differentiation. *Development* **124**, 381-389.

Long, S., Ahmad, N. and Rebagliati, M. R. (2003). The zebrafish nodal-related gene southpaw is required for visceral and diencephalic left-right asymmetry. *Development* **130**, 2303-2316.

Massagué, J. (2000). How cells read TGFβ signals. *Nat. Rev.* **1**, 169-178.

Massagué, J., Seoane, J. and Wotton, D. (2005). Smad transcription factors. *Genes Dev.* **19**, 2783-2810.

Matsui, T., Raya, A., Kawakami, Y., Callol, C., Capdevila, J., Rodriguez-Esteban, C. and Izpisua Belmonte, J. C. (2005). Non-canonical Wnt signaling regulates midline convergence of organ primordia during zebrafish development. *Genes Dev.* **19**, 164-175.

Meno, C., Gritsman, K., Ohishi, S., Ohfuji, Y., Heckscher, E., Mochida, K., Shimono, A., Kondoh, H., Talbot, W. S., Robertson, E. J. et al. (1999). Mouse Lefty2 and zebrafish antivin are feedback inhibitors of nodal signaling during vertebrate gastrulation. *Mol. Cell* **4**, 287-298.

Muller, F., Blader, P., Rastegar, S., Fischer, N., Knochel, W. and Strahle, U. (1999). Characterization of zebrafish smad1, smad2 and smad5: the amino-terminus of smad1 and smad5 is required for specific function in the embryo. *Mech. Dev.* **88**, 73-88.

Nagarajan, R. P. and Chen, Y. (2000). Structural basis for the functional difference between Smad2 and Smad3 in FAST-2 (forkhead activin signal transducer-2)-mediated transcription. *Biochem. J.* **350**, 253-259.

Nasevicius, A. and Ekker, S. C. (2000). Effective targeted gene knockdown in zebrafish. *Nat. Genet.* **26**, 216-220.

Nonaka, S., Yoshiba, S., Watanabe, D., Ikeuchi, S., Goto, T., Marshall, W. F. and Hamada, H. (2005). De novo formation of left-right asymmetry by posterior tilt of nodal cilia. *PLoS Biol.* **3**, e268.

Odenthal, J. and Nüsslein-Volhard, C. (1998). Fork head domain genes in zebrafish. *Dev. Genes Evol.* **208**, 245-258.

Okada, Y., Takeda, S., Tanaka, Y., Izpisúa Belmonte, J. C. and Hirokawa, N. (2005). Mechanism of Nodal flow: A conserved symmetry breaking event in left-right axis determination. *Cell* **121**, 633-644.

Pei, H., Yordy, J. S., Leng, Q., Zhao, Q., Watson, D. K. and Li, R. (2003). EAPII interacts with ETS1 and modulates its transcriptional function. *Oncogene* **22**, 2699-2709.

Peinado, H., Quintanilla, M. and Cano, A. (2003). Transforming growth factor β-1 induces snail transcription factor in epithelial cell lines. *J. Biol. Chem.* **278**, 21113-21123.

Phanish, M. K., Wahab, N. A., Colville-Nash, P., Hendry, B. M. and Dockrell, M. E. (2006). The differential role of Smad2 and Smad3 in the regulation of pro-fibrotic TGFbeta1 responses in human proximal-tubule epthelial cells. *Biochem. J.* **393**, 601-607.

Pogoda, H. M. and Meyer, D. (2002). Zebrafish smad7 is regulated by smad3 and bmp signals. *Dev. Dyn.* **224**, 334-349.

Pogoda, H. M., Solnica-Krezel, L., Driever, W. and Meyer, D. (2000). The zebrafish forkhead transcription factor FoxH1/Fast1 is a modulator of nodal signaling required for organizer formation. *Curr. Biol.* **10**, 1041-1049.

Pype, S., Declercq, W., Ibrahimi, A., Michiels, C., Van Rietschoten, J. G. I., Dewulf, N., de Boer, M., Vandenabeele, P., Huylebroeck, D. and Remacle, J. E. (2000). TTRAP, a novel protein that associates with CD40, Tumor Necrosis Factor (TNF) Receptor-75 and TNF Receptor-associated Factors (TRAFs) and that inhibits Nuclear Factor-κB activation. *J. Biol. Chem.* **275**, 18586-18593.

Rana, A. A., Collart, C., Gilchrist, M. J. and Smith, J. C. (2006). Defining synphenotype groups in Xenopus tropicalis by use of antisense morpholino oligonucleotides. *PLoS Genet.* **11**, e193.

Raya, A. and Belmonte, J. C. I. (2004). Sequential transfer of left-right information during vertebrate development. *Curr. Opin. Genet. Dev.* **14**, 575-581.

Raya, A. and Belmonte, J. (2006). Left-right asymmetry in the vertebrate embryo: from early information to higher-level integration. *Nat. Rev. Genet.* **7**, 283-293.

Rebagliati, M. R., Toyama, R., Haffter, P. and Dawid, I. B. (1998a). Cyclops encodes a nodal-related factor involved in midline signaling. *Proc. Natl. Acad. Sci. USA* **95**, 9932-9937.

Rebagliati, M. R., Toyama, R., Fricke, C., Haffter, P. and Dawid, I. B. (1998b). Zebrafish nodal-related genes are implicated in axial patterning and establishing left-right asymmetry. *Dev. Biol.* **199**, 261-272.

Reissmann, E., Jörnvall, H., Blokzijl, A., Andersson, O., Chang, C., Minchiotti, G., Persico, M. G., Ibanez, C. F. and Brivanlou, A. H. (2001). The orphan receptor ALK7 and the Activin receptor ALK4 mediate signaling by Nodal proteins during vertebrate development. *Genes Dev.* **15**, 2010-2022.

Rodrigues-Lima, F., Josephs, M., Katan, M. and Cassinat, B. (2001). Sequence analysis identifies TTRAP, a protein that associates with CD40 and TNF Receptor-associated factors, as a member of the superfamily of divalent cation-dependent phosphodiesterases. *Biochem. Biophys. Res. Commun.* **285**, 1274-1279.

Roessler, E. and Muenke, M. (2001). Midline and laterality defects, left and right meet in the middle. *BioEssays* **23**, 888-900.

Schier, A. F. (2003). Nodal signaling in vertebrate development. *Annu. Rev. Cell Dev. Biol.* **19**, 589-621.

Schier, A. F., Neuhauss, S. C., Helde, K. A., Talbot, W. S. and Driever, W. (1997). The one-eyed pinhead gene functions in mesoderm and endoderm formation in zebrafish and interacts with no tail. *Development* **124**, 327-342.

Schilling, T. F., Concordet, J. P. and Ingham, P. W. (1999). Regulation of left-right asymmetries in the zebrafish by shh and bmp4. *Dev. Biol.* **210**, 277-287.

Shimizu, T., Yabe, T., Muraoka, O., Yonemura, S., Aramaki, S., Hatta, K., Bae, Y. K., Nojima, H. and Hibi, M. (2005). E-cadherin is required for gastrulation movements in zebrafish. *Mech. Dev.* **122**, 747-763.

Shiratori, H. and Hamada, H. (2006). The left-right axis in the mouse: from origin to morphology. *Development* **133**, 2095-2104.

Sirotkin, H. I., Gates, M. A., Kelly, P. D., Schier, A. F. and Talbot, W. S. (2000).

Fast1 is required for the development of dorsal axial structures in zebrafish. *Curr. Biol.* **10**, 1051-1054. [Erratum in: *Curr. Biol.* **11**, 1643.]

Stainier, D. Y. R., Fouquet, B., Chen, J. N., Warren, K. S., Weinstein, B. M., Meiler, S., Mohideen, M. A., Neuhasuss, S. C., Solnica-Krezel, L., Schier, A. F. et al. (1996). Mutations affecting the formation and function of the cardiovascular system in the zebrafish embryo. *Development* **123**, 285-292.

Stemple, D. L. (2000). Vertebrate development: the fast track to nodal signalling. *Curr. Biol.* **10**, R843-R846.

Summerton, J. and Weller, D. (1997). Morpholino antisense oligomers: design, preparation, and properties. *Antisense Nucleic Acid Drug Dev.* **7**, 187-195.

Tabin, C. J. and Vogan, K. J. (2003). A two-cilia model for vertebrate left-right axis specification. *Genes Dev.* **17**, 1-6.

Thisse, B., Pflumio, S., Fürthauer, M., Loppin, B., Heyer, V., Degrave, A., Woehl, R., Lux, A., Steffan, T., Charbonnier, X. Q. et al. (2001). Expression of the zebrafish genome during embryogenesis (NIH R01 RR15402). ZFIN Direct Data Submission. ZDB-PUB-010810-1.

Toyama, R., O'Connell, M. L., Wright, C. V., Kuehn, M. R. and Dawid, I. B. (1995). Nodal induces ectopic goosecoid and lim1 expression and axis duplication in zebrafish. *Development* **121**, 383-391.

Uemura, M., Swenson, E. S., Gaca, M. D., Giordano, F. J., Reiss, M. and Wells, R. G. (2005). Smad2 and Smad3 play different roles in rat hepatic stellate cell function and alpha-smooth muscle actin organization. *Mol. Biol. Cell* **16**, 4214-4224.

Ulrich, F., Krieg, M., Schotz, E. M., Link, V., Castanon, I., Schnabel, V., Taubenberger, A., Mueller, D., Puech, P. H. and Heisenberg, C. P. (2005). Wnt11 functions in gastrulation by controlling cell cohesion through Rab5c and E-cadherin. *Dev. Cell* **9**, 555-564.

van Grunsven, L. A., Verstappen, G., Huylebroeck, D. and Verschueren, K. (2005). Smads and chromatin modulation. *Cytokine Growth Factor Rev.* **16**, 495-512.

Wang, W., Huang, X. R., Canlas, E., Oka, K., Truong, L. D., Deng, C., Bhowmick, N. A., Ju, W., Bottinger, E. P. and Lan, H. Y. (2006). Essential role of Smad3 in angiotensin II-induced vascular fibrosis. *Circ. Res.* **98**, 1032-1039.

Weinberg, E. S., Allende, M. L., Kelly, C. S., Abdelhamid, A., Murakami, T., Andermann, P., Doerre, O. G., Grunwald, D. J. and Riggleman, B. (1996). Developmental regulation of zebrafish MyoD in wild-type, *no tail* and *spadetail* embryos. *Development* **122**, 271-280.

Westerfield, M. (1995). *The Zebrafish Book: A Guide for the Laboratory use of Zebrafish (Danio rerio)* (4th edn). Eugene, OR: University of Oregon Press.

Whitman, M. (2001). Nodal signaling in early vertebrate embryos: themes and variations. *Dev. Cell* **1**, 605-617.

Whitman, M. and Mercola, M. (2001). TGFbeta superfamily signaling and left-right asymmetry. *Sci. STKE* **64**, RE1.

Yamamoto, A., Amacher, S. L., Kim, S. H., Geissert, D., Kimmel, C. B. and De Robertis, E. M. (1998). Zebrafish paraxial protocadherin is a downstream target of spadetail involved in morphogenesis of gastrula mesoderm. *Development* **125**, 3389-3397.

Yelon, D., Horne, S. A. and Stainier, D. Y. (1999). Restricted expression of cardiac myosin genes reveals regulated aspects of heart tube assembly in zebrafish. *Dev. Biol.* **214**, 23-37.

Yeo, C. Y., Chen, X. and Whitman, M. (1999). The role of FAST-1 and Smads in transcriptional regulation by Activin during early *Xenopus* embryogenesis. *J. Biol. Chem.* **274**, 26584-26590.

Yew, K. H., Prasadan, K. L., Preuett, B. L., Hembree, M. J., McFall, C. R., Benjes, C. L., Crowley, A. R., Sharp, S. L., Li, Z., Tulachan, S. S. et al. (2004). Interplay of glucagon-like peptide-1 and transforming growth factor-beta signaling in insulin-positive differentiation of AR42J cells. *Diabetes* **53**, 2824-2835.

Yost, H. J. (2003). Left-right asymmetry: nodal cilia make and catch a wave. *Curr. Biol.* **13**, R808-R809.

Zhang, J., Talbot, W. S. and Schier, A. F. (1998). Positional cloning identifies zebrafish one-eyed pinhead as a permissive EGF-related ligand required during gastrulation. *Cell* **92**, 241-251.

Table S1. Morpholinos used in this study

Morpholino name	Morpholino sequence 5′ to 3′	Morpholino target	Target sequence or reference
Ttrap[MO1]	TTAAAGCTCTCTCCATGTCCCACTC	Zebrafish Ttrap ORF	+142 to +166
Ttrap[MO2]	CGCTGTCCGATCCAGATACAAAGGC	Zebrafish Ttrap ORF	+88 to +112
Ttrap[ATGMO]	TACCTGACAAAACAGTGTTGGACAT	Zebrafish Ttrap ORF	+1 to +25
Ttrap[SCMO]	CTCTACTTGTTTACCCAAGCCA	(Scrambled control)	(Scrambled sequence of Ttrap[MO1])
Smad3b[MO]	GGCGTGAAAGGCAATATAGACATCT	Zebrafish Smad3b ORF	+1 to +25
Smad2[MO]	GAGTGAAAGGCAAGATGGAGGACAT	Zebrafish Smad2 ORF	+1 to +25
Cadherin1[MO]	AAGCATTTCTCACCTCTCTGTCCAG	Zebrafish cadherin1 ORF	(Kane et al., 2005)
Snail1a[MO]	ATCAGTCCACTCCAGTTACTTTCAG	Zebrafish snail1a ORF	(www.gene-tools.com)
St. fl. control[MO]	CCTCTTACCTCAGTTACAATTTATA	Human β-globin SD (standard fluorescein-labeled control)	(www.gene-tools.com)

Data shown for general knockdowns (to induce LR asymmetry defects) were generated using 4 ng Ttrap MO1. Data shown for general knockdowns (to induce gastrulation and KV defects) were generated using 8 ng each of a 1:1 ratio of Ttrap MO1 and MO2. Data shown for DFC-specific knockdowns to induce LR asymmetry and KV defects were obtained using 8 ng each of a 1:1 ratio of Ttrap MO1 and MO2. For the purpose of simplicity, single Ttrap MO1 and the combination of MO1 and MO2 are all referred to as Ttrap[MO] in main text. ATG-MO was also tested as an additional positive to determine MO specificity, but was otherwise not used in this study owing to lower efficacy (i.e. lower penetrance of LR phenotype/s at similar concentrations as MO1 and MO2).

Table S2. Effect of three Ttrap morpholinos on heart looping

Assay	Stage	MO	Dose	Total n	Normal	Reverse	No Looping	Cardia Bifida	Rudiments*	χ^2	$P \leqslant$
Live	48 hpf	Control MO	16 ng	105	100%	0%	0%	0%	0%		
		Ttrap MO1	4 ng	22	59%	9%	32%	0%	0%	38.4	0.001
			8 ng	37	5%	5%	46%	0%	5%		
		Ttrap MO2	4 ng	23	65%	9%	22%	0%	4%	37.4	0.001
			8 ng	28	32%	36%	25%	0%	7%		
		Ttrap ATGMO	4 ng	42	98%	2%	0%	0%	0%	35.7	0.001
			8 ng	41	85%	12%	2%	0%	0%		

Direction of heart looping and/or *cardia bifida* was scored in live embryos at 48 hpf. Embryos were injected at 1- to 2-cell stages with either scrambled control MO (16 ng), or one of three non-overlapping MOs targeting zebrafish Ttrap at 4 and 8 ng each. *The term 'rudiments' is used for hearts that were strongly reduced in size, had no clearly discernable chambers, had not descended down onto the yolk sac, and were often only recognizable as 'hearts' owing to their contractile behavior. These defects, as well as the *cardia bifida* phenotype precluded ability to score for direction of heart looping or jogging. Statistical analysis was performed using Chi-square analysis: TtrapMO vs control MO; total no. of normal embryos vs total no. of embryos with looping defects.

Table S3. Effect of three Ttrap morpholinos on gastrulation

Assay	Stage	Morpholino	Dose	Total n	Normal	Thickened germ ring	χ^2	$P\leqslant$
Live	Shield	Control MO	16 ng	79	100%	0%		
		Ttrap MO1	4 ng	24	75%	25%	8.5	0.05
			8 ng	37	68%	32%		
		Ttrap MO2	4 ng	25	80%	20%	6.6	0.05
			8 ng	28	71%	29%		
		Ttrap ATGMO	4 ng	22	91%	9%	10.0	0.01
			8 ng	22	64%	36%		

The degree of germ ring thickening was scored in live embryos at shield stage. Embryos were injected at 1- to 2-cell stages with either scrambled control MO (16 ng), or one of three non-overlapping MOs targeting zebrafish Ttrap at 4 and 8 ng each. Statistical analysis was performed using Chi-square analysis: TtrapMO vs. control MO; total no. of normal embryos vs. total no. of embryos with germ-ring defects.

Table S4. Human *TTRAP* mRNA rescues Ttrap morpholino-induced gastrulation defects

Experiment	Assay	Stage	Morpholino + RNA	Dose	Total *n*	Normal	Thick GR	% Rescue
1	Live	Shield	Ttrap MO + huTTRAP	8 ng + 0 pg	54	63%	37%	n/a
				0 ng + 300 pg	52	81%	19%	n/a
				8 ng + 300 pg	52	81%	19%	49%
2	Live	Shield	Ttrap MO + huTTRAP	8 ng + 0 pg	42	62%	38%	n/a
				0 ng + 300 pg	41	78%	22%	n/a
				8 ng + 300 pg	39	90%	10%	74%

Two separate experiments demonstrating partial rescue of Ttrap MO gastrulation phenotype with human *TTRAP* mRNA co-expression. Ttrap MO (8 ng) or hu *TTRAP* mRNA (300 pg) were injected into 1- to 2-cell stage embryos either alone or together, and scored for the thickened germ ring phenotype at shield stage. The lack of sufficient 5' UTR sequence obtainable for zebrafish *ttrap* cDNA precluded the design and synthesis of MOs that targeted regions upstream of the ATG. Since all Ttrap MOs bound to sequences within the coding region, it was not possible to generate an MO-insensitive zebrafish *ttrap* mRNA. We therefore opted to perform the rescues using full-length human *TTRAP* mRNA. n/a, not applicable.

Table S5. DFC-specific *smad3b* mRNA overexpression randomizes direction of heart looping

Assay	Stage	RNA	Dose	Total *n*	Normal	Reverse	No looping	Cardia bifida	Rudiments*	χ^2	$P\leq$
Live	48 hpf	beta-gal	700 pg	93	98%	1%	1%	0%	0%	12.6	0.001
		Smad3b	700 pg	90	82%	7%	9%	0%	2%		

Direction of heart looping and/or cardia bifida was scored in live embryos at 48 hpf. Embryos were injected at 1- to 2-cell stages with either β-galactosidase mRNA (700 pg), or zebrafish smad3b mRNA (700 pg). *The term 'rudiments' is used for hearts that were strongly reduced in size, had no clearly discernable chambers, had not descended down onto the yolk sac, and were often only recognizable as 'hearts' owing to their contractile behavior. These defects precluded ability to score for direction of heart looping or jogging. Statistical analysis was performed using Chi-square analysis: beta-gal DFCoe vs controlDFCoe; total no. of normal embryos vs. total no. of embryos with looping defects. Data presented is combined from two experiments. oe, mRNA overexpression.

Table S6. Smad3 knockdown rescues Ttrap knockdown-induced epiboly defects

Assay	Stage	Morpholino	Dose	Total *n*	Normal	Epiboly defects	Rescue
Live	Tailbud	Ttrap MO	16 ng	23	66%	34%	n/a
		Ttrap MO + Smad3b MO	16 ng + 1 ng	26	90%	10%	70%
		Ttrap MO + Smad3b MO	16 ng + 2 ng	24	80%	20%	41%

Epiboly defects were scored in live embryos at tailbud stage. Embryos were injected at 1- to 2-cell stages with either Ttrap MO alone (16 ng), or together with Smad3b MO (1 or 2 ng). Simultaneous MO-mediated knockdown of Smad3b and Ttrap can partially rescue single Ttrap knockdown phenotype.

Table S7. Smad3 knockdown rescues Ttrap knockdown-induced CE defects

Assay	Stage	Morpholino	Dose	Total *n*	Normal	CE Defects	Rescue
myod	5-9 ss	Ttrap MO	16 ng	20	66%	34%	n/a
		Ttrap MO + Smad3b MO	16 ng + 1 ng	22	79%	21%	37%
		Ttrap MO + Smad3b MO	16 ng + 2 ng	25	86%	14%	59%

Convergent extension defects were scored in fixed embryos stained for myod via whole-mount in situ hybridization at 5-9 somites stages. Embryos were injected at 1- to 2-cell stages with either Ttrap MO alone (16 ng), or together with Smad3b MO (1 or 2 ng). Simultaneous MO-mediated knockdown of Smad3b and Ttrap can partially rescue single Ttrap knockdown phenotype.

Table S8. Smad3 knockdown rescues Ttrap knockdown-induced KV defects

Assay	Stage	Morpholino	Dose	Total *n*	Normal	KV Defects	Rescue
Live	5-9 ss	Ttrap MO	16 ng	60	45%	55%	n/a
		Ttrap MO + Smad3b MO	16 ng + 1 ng	55	65%	35%	37%
		Ttrap MO + Smad3b MO	16 ng + 2 ng	57	67%	33%	39%

KV defects were scored in live embryos at 5- to 9-somite stages. Embryos were injected at 1- to 2-cell stages with either Ttrap MO alone (16 ng), or together with Smad3b MO (1 or 2 ng). Simultaneous MO-mediated knockdown of Smad3b and Ttrap can partially rescue single Ttrap knockdown phenotype.

Table S9. Smad2 knockdown does not rescue Ttrap knockdown-induced CE defects

Assay	Stage	Morpholino	Dose	Total *n*	Normal	CE defects	Rescue
myod	5-9 ss	Ttrap MO	16 ng	40	52%	48%	n/a
		Ttrap MO + Smad2 MO	16 ng + 2 ng	31	52%	48%	0%
		Ttrap MO + Smad2 MO	16 ng + 4 ng	33	12%	88%	–
		Ttrap MO + Smad2 MO	16 ng + 8 ng	32	3%	97%	–

Convergent extension defects were scored in fixed embryos stained for myod via whole mount in situ hybridization at 5- to 9-somite stages. Embryos were injected at 1- to 2-cell stages with either Ttrap MO alone (16 ng), or together with Smad2 MO (2, 4 or 8 ng). Simultaneous MO-mediated knockdown of Smad2 and Ttrap does not rescue single Ttrap knockdown phenotype.

Table S10. Quantification of DFCs in Ttrap^{MO} vs control^{MO} embryos at shield and 70-80% epiboly stages

Treatment	DFC number, shield stage		DFC number, 70-80% epiboly stage	
	Ttrap MO (16 ng)	Control MO (16 ng)	Ttrap MO (16 ng)	Control MO (16 ng)
Embryo total	20	15	19	17
Mean value	20.450	16.230	20.632	25.059
s.d.	4.770	10.000	7.544	8.700
P value	0.095	0.095	0.111	0.111
Significance	NS	NS	NS	NS

There is no significant difference in DFC count between Ttrap^{MO} and Cont^{MO} embryos. Note: DFC number at Bud stage (10 hpf) was not scored due to forming 3D structure of KV at this stage. It was therefore not possible to obtain an accurate cell count in deeper layers of the embryo. Statistical analysis was performed using Student's unpaired *t*-test. NS, not significant.

Table S11. Quantification of DFC sox32/cas domain widths in Ttrap^{MO} vs control^{MO} embryos during gastrulation

	DFC domain width (mm), shield stage		DFC domain width (mm) 70–80% Epiboly		DFC domain width (mm), bud stage	
Treatment	Ttrap MO (16 ng)	Control MO (16 ng)	Ttrap MO (16 ng)	Control MO (16 ng)	Ttrap MO (16 ng)	Control MO (16 ng)
Embryo total	20	15	19	17	23	14
Mean value	0.307	0.2499	0.2551	0.2005	0.1459	0.1016
s.d.	0.089	0.0416	0.0852	0.0640	0.0389	0.0194
P-value	0.029	0.0288	0.0349	0.0349	0.0004	0.0004
Significance	$P \leq 0.05$	$P \leq 0.05$	$P \leq 0.05$	$P \leq 0.05$	$P \leq 0.001$	$P \leq 0.001$

At every stage of gastrulation tested (i.e. shield, 70-80% epiboly, and bud stages), DFC sox32/cas domain widths for Ttrap^{MO} are significantly wider than for control^{MO} embryos.
Statistical analysis was performed using Student's unpaired *t*-test.

Table S12. Double knockdown of Ttrap and Snail1a results in partial rescue of heart looping defects induced by single Ttrap knockdown

%	Wild-type	Ttrap MO only (4 ng)	Ttrap:Snail1a MO (4 ng + 2 ng)
Left looping	94.6	51.6	81.5
Right looping	5.4	29.0	14.8
No looping	0.0	19.4	3.7
Total no. of embryos	37.0	31.0	27.0

One- to two-cell stage embryos were microinjected with either Ttrap MO (4 ng) alone or together with Snail1a MO (2 ng). Wild-type, Ttrap[MO] or Ttrap[MO]:Snail1a[MO] embryos were scored live for direction of heart looping at 48 hpf. Simultaneous knockdown of Snail1a results in partial rescue of single Ttrap knockdown induced heart looping defects. In this experiment, up to 62% of Ttrap[MO] embryos could be rescued. The Snail1a MO sequence used is 5′-ATCAGTCCACTCCAGTTACTTTCAG-3′. This sequence overlaps significantly (21/25 bases) with another Snail1a MO sequence reported previously by Yamashita et al., 2004 (Nature 429:298-302). Note: Ttrap MO dose of 4 ng was chosen because it induces LR defects without gastrulation defects (see Results section of main text). This MO dose also only rarely induces cardia bifida and was therefore not observed in this experiment. Higher doses of Snail1a MO were not tried due to increased death rate by 24 hpf in singly injected Snail1a MO embryos.